MATCH
Communications in Mathematical and in Computer Chemistry

MATCH Commun. Math. Comput. Chem. **67** (2012) 25-54

ISSN 0340 - 6253

Combinatorial Enumeration of Cubane Derivatives as Three-Dimensional Entities. II. Gross Enumeration by the Markaracter Method

Shinsaku Fujita

Shonan Institute of Chemoinformatics and Mathematical Chemistry,

Kaneko 479-7 Ooimachi, Ashigara-Kami-Gun, Kanagawa-Ken,

258-0019 Japan

E-mail: shinsaku_fujita@nifty.com

(Received April 19, 2011)

Abstract

Cubane derivatives with chiral and achiral proligands are counted as 3D structural isomers and as steric isomers in the light of the markaracter method developed by us (S. Fujita, *Theor. Chim. Acta*, **91**, 291–314 (1995), **91**, 315–332 (1995)). The results are further applied to count achiral derivatives as well as enantiomeric pairs of chiral derivatives. The markaracter tables of the point groups $\mathbf{O}_h$ and $\mathbf{O}$, their inverse tables, the dominant USCI-CF (unit subduced cycle indices with chirality fittingness) tables, and the non-dominant USCI-CF tables are prepared for the purpose of further applications of combinatorial enumeration. A Maple program source for calculating non-dominant USCI-CF tables is given as an example of practical calculation.

1 Introduction

In group theory, there are two predominant methodologies which are based on characters and on marks, respectively. They have respective territories, i.e., continuous phenomena for the characters (linked with linear representations [1, 2]) and discrete phenomena for the marks (linked with permutation representations [3, 4]). As a result, they have been studied separately and rather independently in widespread group theory.

Thus, on one hand, the concepts of *character* and *character tables* have been main repertoire of most textbooks on group theory [5, 6], on chemical applications [7–10], on physical applications [11–14], and so on. This is because chemical and physical applications have been concerned with continuous models.

On the other hand, the concepts of *marks* and *mark tables* were early introduced by Burnside [3]. Although they are concerned with permutation groups for specifying discrete phenomena, they have long been neglected in most textbooks on group theory, even on permutation groups [15, 16]. Before and during the 1980s, there had sporadically appeared pioneering articles on the enumeration of graphs and chemical structures by using marks and mark tables [17–19]. After that, the concepts of *marks* and *mark tables* were linked with coset representations of point groups and subductions of such coset representations were formulated [20], so that the concept of *USCI (Unit Subduced Cycle Index)* was proposed by Fujita [20, 21] for the purpose of combinatorial enumeration. After the concepts of *sphericity* and *chirality fittingness* had been introduced by Fujita [22], the concept of USCI was extended into the concept of *USCI-CF (Unit Subduced Cycle Index with Chirality Fittingness)* [23, 24], which has been widely applied to enumeration of three-dimensional structures [21, 25]. In spite of these advances, independent approaches to characters and to marks remained to be unchanged during the first half of the 1990s. This means that the relationship between them were not clarified, so as to be incapable of integrating them from a common viewpoint.

As for the integration of marks and characters, the concept of *markaracters* was proposed later by us [26]. The markaracters are clarified to correspond to dominant representations, which are concerned with cyclic subgroups. Such dominant representations are subduced to give dominant subduction tables. Thereby, dominant USCI tables and non-dominant USCI tables have been generated to be applied to combinatorial enumeration of isomers [27]. The markaracter tables have been correlated to the **Q**-conjugacy character tables, which have been further correlated to character tables [28]. The correlation procedures have been discussed without chirality fittingness, although the method described in [29] could be applied to realize the introduction of chirality fittingness. When both chiral and achiral proligands are incorporated in the enumeration of cubane derivatives as discussed in the present series, chirality fittingness is highly desirable to be taken into consideration.

The purpose of the present series is to compare various methods of combinatorial enumeration, where we use the cubane skeleton of high symmetry ($\mathbf{O}_h$) as a common starting structure and we emphasize three-dimensional structures of enumerated isomers as well as those of ligands to be substituted. In this paper, the markaracter approach is applied to isomer enumerations of cubane derivatives, where both achiral and chiral ligands (more abstractly, proligands) are taken into consideration after introducing chirality fittingness. Thereby, the versatility of the markaracter approach is emphasized even in the cubane skeleton of high symmetry ($\mathbf{O}_h$).

2 Tables for the Point Group $\mathbf{O}_h$

2.1 Markaracter Table of the Point Group $\mathbf{O}_h$

2.1.1 Non-Redundant Set of Cyclic Subgroups

To investigate combinatorial enumeration by starting a cubane skeleton of the point group $\mathbf{O}_h$, we first prepare various tables necessary to the markaracter method [26, 27]. The $\mathbf{O}_h$-point

group is of order 48 and contains the following elements:

$$\begin{aligned}\mathbf{O}_h &= \Big\{I, C_{2(1)}, C_{2(2)}, C_{2(3)}; C_{3(1)}, C_{3(3)}, C_{3(2)}, C_{3(4)}, C^2_{3(1)}, C^2_{3(4)}, C^2_{3(3)}, C^2_{3(2)},\\ &\quad C'_{2(6)}, C'_{2(1)}, C'_{2(4)}, C'_{2(2)}, C'_{2(5)}, C'_{2(3)}, C^3_{4(3)}, C_{4(3)}, C^3_{4(1)}, C_{4(1)}, C_{4(2)}, C^3_{4(2)};\\ &\quad i, \sigma_{h(3)}, \sigma_{h(2)}, \sigma_{h(1)}, S^5_{6(1)}, S^5_{6(3)}, S^5_{6(2)}, S^5_{6(4)}, S_{6(1)}, S_{6(4)}, S_{6(3)}, S_{6(2)},\\ &\quad \sigma_{d(1)}, \sigma_{d(6)}, \sigma_{d(2)}, \sigma_{d(4)}, \sigma_{d(3)}, \sigma_{d(5)}, S_{4(3)}, S^3_{4(3)}, S_{4(1)}, S^3_{4(1)}, S^3_{4(2)}, S_{4(2)}\Big\}. \qquad (1)\end{aligned}$$

The point group $\mathbf{O}_h$ has 33 subgroups up to conjugacy, which have been discussed in detail in terms of a non-redundant set of subgroups (SSG) [30]:

$$\begin{aligned}\mathrm{SSG}_{\mathbf{O}_h} &= \big\{\mathbf{C}_1, \mathbf{C}_2, \mathbf{C}'_2, \mathbf{C}_s, \mathbf{C}'_s, \mathbf{C}_i, \mathbf{C}_3, \mathbf{C}_4, \mathbf{S}_4, \mathbf{D}_2, \mathbf{D}'_2, \mathbf{C}_{2v}, \mathbf{C}'_{2v}, \mathbf{C}''_{2v}, \mathbf{C}_{2h}, \mathbf{C}'_{2h},\\ &\quad \mathbf{D}_3, \mathbf{C}_{3v}, \mathbf{C}_{3i}, \mathbf{D}_4, \mathbf{C}_{4v}, \mathbf{C}_{4h}, \mathbf{D}_{2d}, \mathbf{D}'_{2d}, \mathbf{D}_{2h}, \mathbf{D}'_{2h}, \mathbf{T}, \mathbf{D}_{3d}, \mathbf{D}_{4h}, \mathbf{O}, \mathbf{T}_h, \mathbf{T}_d, \mathbf{O}_h\big\}, \quad (2)\end{aligned}$$

where the subgroups are aligned in the ascending order of their orders. According to the formulation of the USCI approach [21], the respective subgroups correspond to the coset representations $\mathbf{O}_h(/\mathbf{G}_i)$ ($\mathbf{G}_i \in \mathrm{SSG}_{\mathbf{O}_h}$), which generate the corresponding mark table, as reported in Table 1 of [30]. The resulting mark table and its inverse are further used for the subduction of $\mathbf{O}_h(/\mathbf{G}_i) \downarrow \mathbf{G}_j$ ($\mathbf{G}_i, \mathbf{G}_j \in \mathrm{SSG}_{\mathbf{O}_h}$), which results in the generation of the USCI table and the USCI-CF table according to the USCI approach for combinatorial enumeration [21].

Among these subgroups, cyclic subgroups are collected to give a non-redundant set of cyclic subgroups (SCSG) according to [26] as follows:

$$\mathrm{SCSG}_{\mathbf{O}_h} = \big\{\mathbf{C}_1, \mathbf{C}_2, \mathbf{C}'_2, \mathbf{C}_s, \mathbf{C}'_s, \mathbf{C}_i, \mathbf{C}_3, \mathbf{C}_4, \mathbf{S}_4, \mathbf{C}_{3i}\big\}. \qquad (3)$$

The respective subgroups correspond to the coset representations $\mathbf{O}_h(/\mathbf{G}_i)$ ($\mathbf{G}_i \in \mathrm{SCSG}_{\mathbf{O}_h}$), which are selected from the full set of coset representations for $\mathbf{O}_h(/\mathbf{G}_i)$ ($\mathbf{G}_i \in \mathrm{SSG}_{\mathbf{O}_h}$). The restricted set of coset representation, e.g., $\mathbf{O}_h(/\mathbf{G}_i)$ ($\mathbf{G}_i \in \mathrm{SCSG}_{\mathbf{O}_h}$), is called *dominant representations*.

2.1.2 Markaracter Table of $\mathbf{O}_h$ and Its Inverse

Each mark (for $\mathbf{O}_h(/\mathbf{G}_i)$ ($\mathbf{G}_i \in \mathrm{SSG}_{\mathbf{O}_h}$)) can be regarded as a vector of 33 elements (cf. Eq. 2), e.g.,

$$\mathrm{M}_{\mathbf{O}_h(/\mathbf{C}_{3v})} = (8,0,0,0,4,0,2,0,0,0,0,0,0,0,0,0,2,0,0,0,0,0,0,0,0,0,0,0,0,0,0,0) \qquad (4)$$

for the coset representation $\mathbf{O}_h(/\mathbf{C}_{3v})$, which appears in the mark table of the point group $\mathbf{O}_h$ (Table 1 of [30]). In accord with the formulation of markaracters [26], such a mark can be reduced into a markaracter by selecting the values corresponding to the SCSG, e.g., Eq. 3:

$$\widetilde{\mathrm{M}}_{\mathbf{O}_h(/\mathbf{C}_{3v})} = (8,0,0,0,4,0,2,0,0,0), \qquad (5)$$

which is regarded as a vector of 10 elements for the coset representation $\mathbf{O}_h(/\mathbf{C}_{3v})$.

In the present paper, our attention is first focused on markaracters corresponding to SCSG, e.g., $\mathrm{SCSG}_{\mathbf{O}_h}$ (Eq. 3). The markaracters for every coset representations of $\mathbf{O}_h(/\mathbf{G}_i)$ (for $\mathbf{G}_i \in \mathrm{SCSG}_{\mathbf{O}_h}$, cf. Eq. 3) are collected to give a markaracter table shown in Table 1.

In general, a mark table can be converted into a modified mark table by collecting the elements for cyclic subgroups in the upper left part, where the resulting upper left part of the

Table 1: Markaracter Table of $\mathbf{O}_h$

$\widetilde{\mathrm{M}}_{\mathbf{O}_h}$	$\mathbf{C}_1$	$\mathbf{C}_2$	$\mathbf{C}'_2$	$\mathbf{C}_s$	$\mathbf{C}'_s$	$\mathbf{C}_i$	$\mathbf{C}_3$	$\mathbf{C}_4$	$\mathbf{S}_4$	$\mathbf{C}_{3i}$
$\mathbf{O}_h(/\mathbf{C}_1)$	48	0	0	0	0	0	0	0	0	0
$\mathbf{O}_h(/\mathbf{C}_2)$	24	8	0	0	0	0	0	0	0	0
$\mathbf{O}_h(/\mathbf{C}'_2)$	24	0	4	0	0	0	0	0	0	0
$\mathbf{O}_h(/\mathbf{C}_s)$	24	0	0	8	0	0	0	0	0	0
$\mathbf{O}_h(/\mathbf{C}'_s)$	24	0	0	0	4	0	0	0	0	0
$\mathbf{O}_h(/\mathbf{C}_i)$	24	0	0	0	0	24	0	0	0	0
$\mathbf{O}_h(/\mathbf{C}_3)$	16	0	0	0	0	0	4	0	0	0
$\mathbf{O}_h(/\mathbf{C}_4)$	12	4	0	0	0	0	0	4	0	0
$\mathbf{O}_h(/\mathbf{S}_4)$	12	4	0	0	0	0	0	0	4	0
$\mathbf{O}_h(/\mathbf{C}_{3i})$	8	0	0	0	0	8	2	0	0	2

Table 2: Inverse Markaracter Table of $\mathbf{O}_h$

$\widetilde{\mathrm{M}}^{-1}_{\mathbf{O}_h}$	$\mathbf{O}_h$ $(/\mathbf{C}_1)$	$\mathbf{O}_h$ $(/\mathbf{C}_2)$	$\mathbf{O}_h$ $(/\mathbf{C}'_2)$	$\mathbf{O}_h$ $(/\mathbf{C}_s)$	$\mathbf{O}_h$ $(/\mathbf{C}'_s)$	$\mathbf{O}_h$ $(/\mathbf{C}_i)$	$\mathbf{O}_h$ $(/\mathbf{C}_3)$	$\mathbf{O}_h$ $(/\mathbf{C}_4)$	$\mathbf{O}_h$ $(/\mathbf{S}_4)$	$\mathbf{O}_h$ $(/\mathbf{C}_{3i})$	Σ
$\mathbf{C}_1$	$\frac{1}{48}$	0	0	0	0	0	0	0	0	0	$\frac{1}{48}$
$\mathbf{C}_2$	$-\frac{1}{16}$	$\frac{1}{8}$	0	0	0	0	0	0	0	0	$\frac{1}{16}$
$\mathbf{C}'_2$	$-\frac{1}{8}$	0	$\frac{1}{4}$	0	0	0	0	0	0	0	$\frac{1}{8}$
$\mathbf{C}_s$	$-\frac{1}{16}$	0	0	$\frac{1}{8}$	0	0	0	0	0	0	$\frac{1}{16}$
$\mathbf{C}'_s$	$-\frac{1}{8}$	0	0	0	$\frac{1}{4}$	0	0	0	0	0	$\frac{1}{8}$
$\mathbf{C}_i$	$-\frac{1}{48}$	0	0	0	0	$\frac{1}{24}$	0	0	0	0	$\frac{1}{48}$
$\mathbf{C}_3$	$-\frac{1}{12}$	0	0	0	0	0	$\frac{1}{4}$	0	0	0	$\frac{1}{6}$
$\mathbf{C}_4$	0	$-\frac{1}{8}$	0	0	0	0	0	$\frac{1}{4}$	0	0	$\frac{1}{8}$
$\mathbf{S}_4$	0	$-\frac{1}{8}$	0	0	0	0	0	0	$\frac{1}{4}$	0	$\frac{1}{8}$
$\mathbf{C}_{3i}$	$\frac{1}{12}$	0	0	0	0	$-\frac{1}{6}$	$-\frac{1}{4}$	0	0	$\frac{1}{2}$	$\frac{1}{6}$

modified mark table indicates the corresponding markaracter table [26]. By applying this procedure to the present case, the mark table of $\mathbf{O}_h$ reported in [30] (Table 1) is converted into the corresponding modified mark table, in which the markaracter table (Table 1) appears in its upper left part.

2.1.3 Dominant USCI-CF Table of $\mathbf{O}_h$

In general, dominant representations such as $\mathbf{O}_h(/\mathbf{G}_i)$ ($\mathbf{G}_i \in \mathrm{SCSG}_{\mathbf{O}_h}$) (corresponding to the SCSG (Eq. 3)) can be subduced into a cyclic subgroup, where the resulting subductions generate dominant USCIs [27]. Although the reference [27] has solely discussed dominant USCIs *without* chirality fittingness, the corresponding USCI-CFs (with chirality fittingness) can be derived by referring to the formulation of the USCI approach (cf. Chapter 19 of [21]).

As an example, let us consider the subductions of $\mathbf{O}_h(/\mathbf{G}_i)$ ($\mathbf{G}_i \in \mathrm{SCSG}_{\mathbf{O}_h}$) into the cyclic subgroup $\mathbf{S}_4$. According to the procedure described in Example 4 of [27], a subduced markaracter table is generated by selecting necessary columns ($\mathbf{C}_1$-, $\mathbf{C}_2$-, and $\mathbf{S}_4$-columns) from the markaracter table (Table 1). The resulting matrix (the subduced markaracter table for $\mathbf{O}_h(/\mathbf{G}_i)\downarrow \mathbf{S}_4$ ($\mathbf{G}_i \in \mathrm{SCSG}_{\mathbf{O}_h}$)) is multiplied by the inverse ($\widetilde{\mathrm{M}}^{-1}_{\mathbf{S}_4}$, the same as the inverse of the mark table $\mathrm{M}^{-1}_{\mathbf{S}_4}$, cf. Table B.4 of Appendix B in [21]) to give a subduction-multiplicity matrix as follows:

$$
\begin{array}{c}
\\
\mathbf{O}_h(/\mathbf{C}_1)\\
\mathbf{O}_h(/\mathbf{C}_2)\\
\mathbf{O}_h(/\mathbf{C}'_2)\\
\mathbf{O}_h(/\mathbf{C}_s)\\
\mathbf{O}_h(/\mathbf{C}'_s)\\
\mathbf{O}_h(/\mathbf{C}_i)\\
\mathbf{O}_h(/\mathbf{C}_3)\\
\mathbf{O}_h(/\mathbf{C}_4)\\
\mathbf{O}_h(/\mathbf{S}_4)\\
\mathbf{O}_h(/\mathbf{C}_{3i})
\end{array}
\begin{array}{c}
\begin{array}{ccc} \mathbf{C}_1 & \mathbf{C}_2 & \mathbf{S}_4 \end{array}\\
\begin{pmatrix}
48 & 0 & 0\\
24 & 8 & 0\\
24 & 0 & 0\\
24 & 0 & 0\\
24 & 0 & 0\\
24 & 0 & 0\\
16 & 0 & 0\\
12 & 4 & 0\\
12 & 4 & 4\\
8 & 0 & 0
\end{pmatrix}
\end{array}
\begin{pmatrix}
\frac{1}{4} & 0 & 0\\
-\frac{1}{4} & \frac{1}{2} & 0\\
0 & -\frac{1}{2} & 1
\end{pmatrix}
=
\begin{array}{c}
\\
\mathbf{O}_h(/\mathbf{C}_1)\downarrow \mathbf{S}_4\\
\mathbf{O}_h(/\mathbf{C}_2)\downarrow \mathbf{S}_4\\
\mathbf{O}_h(/\mathbf{C}'_2)\downarrow \mathbf{S}_4\\
\mathbf{O}_h(/\mathbf{C}_s)\downarrow \mathbf{S}_4\\
\mathbf{O}_h(/\mathbf{C}'_s)\downarrow \mathbf{S}_4\\
\mathbf{O}_h(/\mathbf{C}_i)\downarrow \mathbf{S}_4\\
\mathbf{O}_h(/\mathbf{C}_3)\downarrow \mathbf{S}_4\\
\mathbf{O}_h(/\mathbf{C}_4)\downarrow \mathbf{S}_4\\
\mathbf{O}_h(/\mathbf{S}_4)\downarrow \mathbf{S}_4\\
\mathbf{O}_h(/\mathbf{C}_{3i})\downarrow \mathbf{S}_4
\end{array}
\begin{array}{c}
\begin{array}{ccc} \mathbf{C}_1 & \mathbf{C}_2 & \mathbf{S}_4 \end{array}\\
\begin{pmatrix}
12 & 0 & 0\\
4 & 4 & 0\\
6 & 0 & 0\\
6 & 0 & 0\\
6 & 0 & 0\\
6 & 0 & 0\\
4 & 0 & 0\\
2 & 2 & 0\\
2 & 0 & 4\\
2 & 0 & 0
\end{pmatrix}
\end{array}
\begin{array}{c}
\\
c_4^{12}\\
c_2^4 c_4^4\\
c_4^6\\
c_4^6\\
c_4^6\\
c_4^6\\
c_4^4\\
c_2^2 c_4^2\\
a_1^4 c_4^2\\
c_4^2
\end{array}
\quad , \qquad (6)
$$

where the first matrix in the left-hand side is the the subduced markaracter table at issue, the second one is $\widetilde{\mathrm{M}}^{-1}_{\mathbf{S}_4}$, and the matrix in the right-hand side is the subduction-multiplicity matrix at issue.

The subduction-multiplicity matrix (the right-hand side of Eq. 6) contains the multiplicities for the respective subductions. For example, the 9-th row indicates:

$$\mathbf{O}_h(/\mathbf{S}_4)\downarrow \mathbf{S}_4 = 2\mathbf{S}_4(/\mathbf{C}_1) + 4\mathbf{S}_4(/\mathbf{S}_4). \qquad (7)$$

Equation 7 generates a USCI $s_1^4 s_4^2$, because the subscripts are calculated by using $|\mathbf{S}_4|/|\mathbf{C}_1| = 4/1 = 4$ and $|\mathbf{S}_4|/|\mathbf{S}_4| = 4/4 = 1$, where the coefficients appearing in the right-hand side are used as the powers of the respective components of the USCI. Because the $\mathbf{S}_4(/\mathbf{C}_1)$ is enantiospheric and because the $\mathbf{S}_4(/\mathbf{S}_4)$ is homospheric in accord with the USCI approach [21], they are respectively characterized by the sphericity indices c_4 and a_1. Hence a USCI-CF is calculated to be $a_1^4 c_4^2$. This is symbolically denoted as follows:

$$\mathrm{Z}(\mathbf{O}_h(/\mathbf{S}_4)\downarrow \mathbf{S}_4; \$_{d_{jk}}) = a_1^4 c_4^2. \qquad (8)$$

Table 3: Dominant USCI-CF Table of $\mathbf{O}_h$

	$\mathbf{C}_1$	$\mathbf{C}_2$	$\mathbf{C}'_2$	$\mathbf{C}_s$	$\mathbf{C}'_s$	$\mathbf{C}_i$	$\mathbf{C}_3$	$\mathbf{C}_4$	$\mathbf{S}_4$	$\mathbf{C}_{3i}$
$\mathbf{O}_h(/\mathbf{C}_1)$	b_1^{48}	b_2^{24}	b_2^{24}	c_2^{24}	c_2^{24}	c_2^{24}	b_3^{16}	b_4^{12}	c_4^{12}	c_6^8
$\mathbf{O}_h(/\mathbf{C}_2)$	b_1^{24}	$b_1^8 b_2^8$	b_2^{12}	c_2^{12}	c_2^{12}	c_2^{12}	b_3^8	$b_2^4 b_4^4$	$c_2^4 c_4^4$	c_6^4
$\mathbf{O}_h(/\mathbf{C}'_2)$	b_1^{24}	b_2^{12}	$b_1^4 b_2^{10}$	c_2^{12}	c_2^{12}	c_2^{12}	b_3^8	b_4^6	c_4^6	c_6^4
$\mathbf{O}_h(/\mathbf{C}_s)$	b_1^{24}	b_2^{12}	b_2^{12}	$a_1^8 c_2^8$	c_2^{12}	c_2^{12}	b_3^8	b_4^6	c_4^6	c_6^4
$\mathbf{O}_h(/\mathbf{C}'_s)$	b_1^{24}	b_2^{12}	b_2^{12}	c_2^{12}	$a_1^4 c_2^{10}$	c_2^{12}	b_3^8	b_4^6	c_4^6	c_6^4
$\mathbf{O}_h(/\mathbf{C}_i)$	b_1^{24}	b_2^{12}	b_2^{12}	c_2^{12}	c_2^{12}	a_1^{24}	b_3^8	b_4^6	c_4^6	a_3^8
$\mathbf{O}_h(/\mathbf{C}_3)$	b_1^{16}	b_2^8	b_2^8	c_2^8	c_2^8	c_2^8	$b_1^4 b_3^4$	b_4^4	c_4^4	$c_2^2 c_6^2$
$\mathbf{O}_h(/\mathbf{C}_4)$	b_1^{12}	$b_1^4 b_2^4$	b_2^6	c_2^6	c_2^6	c_2^6	b_3^4	$b_1^4 b_4^2$	$c_2^2 c_4^2$	c_6^2
$\mathbf{O}_h(/\mathbf{S}_4)$	b_1^{12}	$b_1^4 b_2^4$	b_2^6	c_2^6	c_2^6	c_2^6	b_3^4	$b_2^2 b_4^2$	$a_1^4 c_4^2$	c_6^2
$\mathbf{O}_h(/\mathbf{C}_{3i})$	b_1^8	b_2^4	b_2^4	c_2^4	c_2^4	a_1^8	$b_1^2 b_3^2$	b_4^2	c_4^2	$a_1^2 a_3^2$
$\sum$	$\frac{1}{48}$	$\frac{1}{16}$	$\frac{1}{8}$	$\frac{1}{16}$	$\frac{1}{8}$	$\frac{1}{48}$	$\frac{1}{6}$	$\frac{1}{8}$	$\frac{1}{8}$	$\frac{1}{6}$

On similar lines, the other subductions are characterized by USCI-CFs collected in the rightmost part of Eq. 6.

The subduction procedure described in the preceding paragraphs is repeated for each cyclic subgroup by selecting the columns necessary to the cyclic subgroup from the markaracter table (Table 1). Thereby, we are able to obtain a dominant USCI-CF table of $\mathbf{O}_h$ (Table 3). Note that the USCI-CFs shown in Eq. 6 appear in the $\mathbf{S}_4$-column of Table 3.

Let a point group $\mathbf{G}$ be characterized by an SCSG:

$$\mathrm{SCSG}_{\mathbf{G}} = \{\mathbf{G}_1, \mathbf{G}_s, \ldots, \mathbf{G}_s\}, \tag{9}$$

where $\mathbf{G}_1 = \mathbf{C}_1$ (an identity group). In general, Eq. 7 is represented as follows:

$$\mathbf{G}(/\mathbf{G}_i) \downarrow \mathbf{G}_j = \sum_{k=1}^{r} \beta_k^{(ij)} \mathbf{G}_j(/\mathbf{G}_k), \tag{10}$$

which has been reported in [27] (Eq. 48). Thereby, Eq. 8 is generally represented as follows:

$$\mathrm{Z}(\mathbf{G}(/\mathbf{G}_i) \downarrow \mathbf{G}_j; \$_{d_{jk}}) = \prod_{k=1}^{r} \$_{d_{jk}}^{\beta_k^{(ij)}}, \tag{11}$$

which represents a USCI-CF appearing at the intersection of the $\mathbf{G}(/\mathbf{G}_i)$-row and $\mathbf{G}_j$ column of the dominant USCI-CF table of $\mathbf{G}$, where k is concerned with $\mathbf{G}_j(/\mathbf{G}_k)$ ($d_{jk} = |\mathbf{G}_j|/|\mathbf{G}_k|$). The symbol \$ is a (for homospheric), b (for hemispheric), or c (for enantiospheric) according to the sphericity of $\mathbf{G}_j(/\mathbf{G}_k)$ (cf. Eq. 50 of [27] without chirality fittingness).

2.2 Markaracters and USCI-CFs for Non-Dominant Representations

2.2.1 Multiplicity Vectors

A markaracter table such as Table 1 is regarded as a square matrix, e.g., $\widetilde{\mathrm{M}}_{\mathbf{O}_h}$. Thereby, we are able to calculate the corresponding inverse matrix, e.g., $\widetilde{\mathrm{M}}^{-1}_{\mathbf{O}_h}$, as shown in Table 2 [26]. As for

the present case, we obtain the following relationship:

$$\widetilde{\mathrm{M}}_{\mathbf{O}_h}\widetilde{\mathrm{M}}_{\mathbf{O}_h}^{-1}=\mathrm{I}_{10\times 10}, \tag{12}$$

where the symbol $\mathrm{I}_{10\times 10}$ represents an identity matrix of 10×10.

Each row of a markaracter table (e.g., Table 1) can be regarded as a row vector according to Theorem 1 of [26]. From this viewpoint, the set of row vectors (i.e., markaracters) can work as the bases of a vector space, where Eq. 12 indicates the multiplicities of respective row vectors. For example, the $\mathbf{O}_h(/\mathbf{C}_2)$-row of Table 1 as a vector is multiplied by the inverse (Table 2) to give the following multiplicity vector:

$$\widetilde{\mathrm{M}}_{\mathbf{O}_h(/\mathbf{C}_2)}\widetilde{\mathrm{M}}_{\mathbf{O}_h}^{-1}=(24,8,0,0,0,0,0,0,0,0)\widetilde{\mathrm{M}}_{\mathbf{O}_h}^{-1}=(0,1,0,0,0,0,0,0,0,0), \tag{13}$$

which corresponds to the $\mathbf{O}_h(/\mathbf{C}_2)$-rows of $\widetilde{\mathrm{M}}_{\mathbf{O}_h}$ and $\mathrm{I}_{10\times 10}$ appearing in Eq. 12. This means that the base $\widetilde{\mathrm{M}}_{\mathbf{O}_h(/\mathbf{C}_2)}$ contains the representation $\mathbf{O}_h(/\mathbf{C}_2)$ once and no other dominant representations. On similar lines, the base $\widetilde{\mathrm{M}}_{\mathbf{O}_h(/\mathbf{G}_i)}$ ($\mathbf{G}_i\in \mathrm{SCSG}_{\mathbf{O}_h}$)) corresponding to each row of Table 1 ($\mathbf{O}_h(/\mathbf{G}_i)$ ($\mathbf{G}_i\in \mathrm{SCSG}_{\mathbf{O}_h}$) as dominant representations) contains the representation $\mathbf{O}_h(/\mathbf{G}_i)$ once and no other dominant representations in the light of Eq. 12.

Now, the discussions described above for such dominant representations as $\mathbf{O}_h(/\mathbf{G}_i)$ ($\mathbf{G}_i\in \mathrm{SCSG}_{\mathbf{O}_h}$) allows us to apply Theorem 1 of of [26] and then Subsection 3.2 of of [27] in order to examine non-dominant representations, e.g., $\mathbf{O}_h(/\mathbf{C}_{3v})$ whose markaracter has been shown in Eq. 5. The markaracter shown in Eq. 5 is regarded as a vector and multiplied by the inverse $\widetilde{\mathrm{M}}_{\mathbf{O}_h}^{-1}$, so as to give the following multiplicity vector:

$$\widetilde{\mathrm{M}}_{\mathbf{O}_h(/\mathbf{C}_{3v})}\widetilde{\mathrm{M}}_{\mathbf{O}_h}^{-1}=(8,0,0,0,4,0,2,0,0,0)\widetilde{\mathrm{M}}_{\mathbf{O}_h}^{-1}=(-\frac{1}{2},0,0,0,1,0,\frac{1}{2},0,0,0). \tag{14}$$

This means the following equation:

$$\widetilde{\mathrm{M}}_{\mathbf{O}_h(/\mathbf{C}_{3v})}=-\frac{1}{2}\widetilde{\mathrm{M}}_{\mathbf{O}_h(/\mathbf{C}_1)}+\widetilde{\mathrm{M}}_{\mathbf{O}_h(/\mathbf{C}'_s)}+\frac{1}{2}\widetilde{\mathrm{M}}_{\mathbf{O}_h(/\mathbf{C}_3)}, \tag{15}$$

which is verified by the data of Table 1 as follows:

$$\begin{array}{rl}
-\frac{1}{2}\times & (48,\ 0,\ 0,\ 0,\ 0,\ 0,\ 0,\ 0,\ 0,\ 0)\\
+1\times & (24,\ 0,\ 0,\ 0,\ 4,\ 0,\ 0,\ 0,\ 0,\ 0)\\
+\frac{1}{2}\times & (16,\ 0,\ 0,\ 0,\ 0,\ 0,\ 4,\ 0,\ 0,\ 0)\\
\hline
 & (\ 8,\ 0,\ 0,\ 0,\ 4,\ 0,\ 2,\ 0,\ 0,\ 0)
\end{array}. \tag{16}$$

Non-dominant representations $\mathbf{O}_h(/\mathbf{G}_i)$ ($\mathbf{G}_i\in \mathrm{SSG}_{\mathbf{O}_h}$ and $\mathbf{G}_i\notin \mathrm{SCSG}_{\mathbf{O}_h}$) can be similarly treated to give respective multiplicity vectors, which are collected in Table 4.

2.2.2 Non-Dominant USCI-CF Table of $\mathbf{O}_h$

Via Multiplicity Vectors Such multiplicity vectors as collected in Table 4, which are initially linked to such a markaracter table as Table 1, can be applied to such a dominant USCI table (or dominant USCI-CF table) as Table 3 according to Theorem 4 of [27]. Thus, the multiplicity vectors (e.g., Table 4) are capable of calculating USCIs (or USCI-CFs) for non-dominant representations by starting from the data of such a dominant USCI (or USCI-CF) table (e.g., Table 3).

Table 4: Markaracters and Multiplicity Vectors for Non-Dominant Representations

markaracter		$\times\widetilde{\mathrm{M}}_{\mathbf{O}_h}^{-1}$	multiplicity vectors
$\widetilde{\mathrm{M}}_{\mathbf{O}_h(/\mathbf{D}_2)}$	$=(12,12,0,0,0,0,0,0,0,0)$	$\Longrightarrow$	$(-\frac{1}{2},\frac{3}{2},0,0,0,0,0,0,0,0)$
$\widetilde{\mathrm{M}}_{\mathbf{O}_h(/\mathbf{D}'_2)}$	$=(12,4,4,0,0,0,0,0,0,0)$	$\Longrightarrow$	$(-\frac{1}{2},\frac{1}{2},1,0,0,0,0,0,0,0)$
$\widetilde{\mathrm{M}}_{\mathbf{O}_h(/\mathbf{C}_{2v})}$	$=(12,4,0,8,0,0,0,0,0,0)$	$\Longrightarrow$	$(-\frac{1}{2},\frac{1}{2},0,1,0,0,0,0,0,0)$
$\widetilde{\mathrm{M}}_{\mathbf{O}_h(/\mathbf{C}'_{2v})}$	$=(12,4,0,0,4,0,0,0,0,0)$	$\Longrightarrow$	$(-\frac{1}{2},\frac{1}{2},0,0,1,0,0,0,0,0)$
$\widetilde{\mathrm{M}}_{\mathbf{O}_h(/\mathbf{C}''_{2v})}$	$=(12,0,2,4,2,0,0,0,0,0)$	$\Longrightarrow$	$(-\frac{1}{2},0,\frac{1}{2},\frac{1}{2},\frac{1}{2},0,0,0,0,0)$
$\widetilde{\mathrm{M}}_{\mathbf{O}_h(/\mathbf{C}_{2h})}$	$=(12,4,0,4,0,12,0,0,0,0)$	$\Longrightarrow$	$(-\frac{1}{2},\frac{1}{2},0,\frac{1}{2},0,\frac{1}{2},0,0,0,0)$
$\widetilde{\mathrm{M}}_{\mathbf{O}_h(/\mathbf{C}'_{2h})}$	$=(12,0,2,0,2,12,0,0,0,0)$	$\Longrightarrow$	$(-\frac{1}{2},0,\frac{1}{2},0,\frac{1}{2},\frac{1}{2},0,0,0,0)$
$\widetilde{\mathrm{M}}_{\mathbf{O}_h(/\mathbf{D}_3)}$	$=(8,0,4,0,0,0,2,0,0,0)$	$\Longrightarrow$	$(-\frac{1}{2},0,1,0,0,0,\frac{1}{2},0,0,0)$
$\widetilde{\mathrm{M}}_{\mathbf{O}_h(/\mathbf{C}_{3v})}$	$=(8,0,0,0,4,0,2,0,0,0)$	$\Longrightarrow$	$(-\frac{1}{2},0,0,0,1,0,\frac{1}{2},0,0,0)$
$\widetilde{\mathrm{M}}_{\mathbf{O}_h(/\mathbf{D}_4)}$	$=(6,6,2,0,0,0,0,2,0,0)$	$\Longrightarrow$	$(-\frac{1}{2},\frac{1}{2},\frac{1}{2},0,0,0,0,\frac{1}{2},0,0)$
$\widetilde{\mathrm{M}}_{\mathbf{O}_h(/\mathbf{C}_{4v})}$	$=(6,2,0,4,2,0,0,2,0,0)$	$\Longrightarrow$	$(-\frac{1}{2},0,0,\frac{1}{2},\frac{1}{2},0,0,\frac{1}{2},0,0)$
$\widetilde{\mathrm{M}}_{\mathbf{O}_h(/\mathbf{C}_{4h})}$	$=(6,2,0,2,0,6,0,2,2,0)$	$\Longrightarrow$	$(-\frac{1}{4},-\frac{1}{4},0,\frac{1}{4},0,\frac{1}{4},0,\frac{1}{2},\frac{1}{2},0)$
$\widetilde{\mathrm{M}}_{\mathbf{O}_h(/\mathbf{D}_{2d})}$	$=(6,6,0,0,2,0,0,0,2,0)$	$\Longrightarrow$	$(-\frac{1}{2},\frac{1}{2},0,0,\frac{1}{2},0,0,0,\frac{1}{2},0)$
$\widetilde{\mathrm{M}}_{\mathbf{O}_h(/\mathbf{D}'_{2d})}$	$=(6,2,2,4,0,0,0,0,2,0)$	$\Longrightarrow$	$(-\frac{1}{2},0,\frac{1}{2},\frac{1}{2},0,0,0,0,\frac{1}{2},0)$
$\widetilde{\mathrm{M}}_{\mathbf{O}_h(/\mathbf{D}_{2h})}$	$=(6,6,0,6,0,6,0,0,0,0)$	$\Longrightarrow$	$(-\frac{3}{4},3/4,0,3/4,0,\frac{1}{4},0,0,0,0)$
$\widetilde{\mathrm{M}}_{\mathbf{O}_h(/\mathbf{D}'_{2h})}$	$=(6,2,2,2,2,6,0,0,0,0)$	$\Longrightarrow$	$(-\frac{3}{4},\frac{1}{4},\frac{1}{2},\frac{1}{4},\frac{1}{2},\frac{1}{4},0,0,0,0)$
$\widetilde{\mathrm{M}}_{\mathbf{O}_h(/\mathbf{T})}$	$=(4,4,0,0,0,0,4,0,0,0)$	$\Longrightarrow$	$(-\frac{1}{2},\frac{1}{2},0,0,0,0,1,0,0,0)$
$\widetilde{\mathrm{M}}_{\mathbf{O}_h(/\mathbf{D}_{3d})}$	$=(4,0,2,0,2,4,1,0,0,1)$	$\Longrightarrow$	$(-\frac{1}{2},0,\frac{1}{2},0,\frac{1}{2},0,0,0,0,\frac{1}{2})$
$\widetilde{\mathrm{M}}_{\mathbf{O}_h(/\mathbf{D}_{4h})}$	$=(3,3,1,3,1,3,0,1,1,0)$	$\Longrightarrow$	$(-\frac{5}{8},\frac{1}{8},\frac{1}{4},\frac{3}{8},\frac{1}{4},1/8,0,\frac{1}{4},\frac{1}{4},0)$
$\widetilde{\mathrm{M}}_{\mathbf{O}_h(/\mathbf{O})}$	$=(2,2,2,0,0,0,2,2,0,0)$	$\Longrightarrow$	$(-\frac{1}{2},0,\frac{1}{2},0,0,0,\frac{1}{2},\frac{1}{2},0,0)$
$\widetilde{\mathrm{M}}_{\mathbf{O}_h(/\mathbf{T}_h)}$	$=(2,2,0,2,0,2,2,0,0,2)$	$\Longrightarrow$	$(-\frac{1}{4},\frac{1}{4},0,\frac{1}{4},0,-\frac{1}{4},0,0,0,1)$
$\widetilde{\mathrm{M}}_{\mathbf{O}_h(/\mathbf{T}_d)}$	$=(2,2,0,0,2,0,2,0,2,0)$	$\Longrightarrow$	$(-\frac{1}{2},0,0,0,\frac{1}{2},0,\frac{1}{2},0,\frac{1}{2},0)$
$\widetilde{\mathrm{M}}_{\mathbf{O}_h(/\mathbf{O}_h)}$	$=(1,1,1,1,1,1,1,1,1,1)$	$\Longrightarrow$	$(-\frac{3}{8},-\frac{1}{8},\frac{1}{4},\frac{1}{8},\frac{1}{4},-\frac{1}{8},0,\frac{1}{4},\frac{1}{4},\frac{1}{2})$

For example, the multiplicity vector of Eq. 14 (for the markaracter $\widetilde{\mathrm{M}}_{\mathbf{O}_h(/\mathbf{C}_{3v})}$) is concerned with the $\mathbf{O}_h(/\mathbf{C}_1)$-, $\mathbf{O}_h(/\mathbf{C}'_s)$-, and $\mathbf{O}_h(/\mathbf{C}_3)$-rows of the dominant USCI-CF table (Table 3), as implied by Eq. 15. From the data of the $\mathbf{S}_4$-column shown in Table 3 as an example, we select c_4^{12} for $\mathbf{O}_h(/\mathbf{C}_1)$-row, c_4^6 for $\mathbf{O}_h(/\mathbf{C}'_s)$-row, and c_4^4 for $\mathbf{O}_h(/\mathbf{C}_3)$-row, to which we apply the multiplicity vector shown in Eq. 14, giving the following USCI-CF:

$$c_4^{12\times(-1/2)} \times c_4^{6\times 1} \times c_4^{4\times(1/2)} = c_4^2. \tag{17}$$

Similarly, the multiplicity vector of Eq. 14 is applied to the other columns of Table 3 so as to give a vector of USCI-CFs for the markaracter $\widetilde{\mathrm{M}}_{\mathbf{O}_h(/\mathbf{C}_{3v})}$, as collected in the $\mathbf{O}_h(/\mathbf{C}_{3v})$-row of Table 5.

The full data of Table 5 can be obtained by repeatedly applying this procedure to the markaracters and the multiplicity vectors collected in Table 4. They were calculated by using the Maple system [31], where a maple file named "markarac04.mpl" (extension .mpl), whose source list

Table 5: Non-Dominant USCI-CF Table of $\mathbf{O}_h$

	$\mathbf{C}_1$	$\mathbf{C}_2$	$\mathbf{C}'_2$	$\mathbf{C}_s$	$\mathbf{C}'_s$	$\mathbf{C}_i$	$\mathbf{C}_3$	$\mathbf{C}_4$	$\mathbf{S}_4$	$\mathbf{C}_{3i}$
$\mathbf{O}_h(/\mathbf{D}_2)$	b_1^{12}	b_1^{12}	b_2^6	c_2^6	c_2^6	c_2^6	b_3^4	b_2^6	c_2^6	c_6^2
$\mathbf{O}_h(/\mathbf{D}'_2)$	b_1^{12}	$b_1^4b_2^4$	$b_1^4b_2^4$	c_2^6	c_2^6	c_2^6	b_3^4	$b_2^2b_4^2$	$c_2^2c_4^2$	c_6^2
$\mathbf{O}_h(/\mathbf{C}_{2v})$	b_1^{12}	$b_1^4b_2^4$	b_2^6	$a_1^8c_2^2$	c_2^6	c_2^6	b_3^4	$b_2^2b_4^2$	$c_2^2c_4^2$	c_6^2
$\mathbf{O}_h(/\mathbf{C}'_{2v})$	b_1^{12}	$b_1^4b_2^4$	b_2^6	c_2^6	$a_1^4c_2^4$	c_2^6	b_3^4	$b_2^2b_4^2$	$c_2^2c_4^2$	c_6^2
$\mathbf{O}_h(/\mathbf{C}''_{2v})$	b_1^{12}	b_2^6	$b_1^2b_2^5$	$a_1^4c_2^4$	$a_1^2c_2^5$	c_2^6	b_3^4	b_4^3	c_4^3	c_6^2
$\mathbf{O}_h(/\mathbf{C}_{2h})$	b_1^{12}	$b_1^4b_2^4$	b_2^6	$a_1^4c_2^4$	c_2^6	a_1^{12}	b_3^4	$b_2^2b_4^2$	$c_2^2c_4^2$	a_3^4
$\mathbf{O}_h(/\mathbf{C}'_{2h})$	b_1^{12}	b_2^6	$b_1^2b_2^5$	c_2^6	$a_1^2c_2^5$	a_1^{12}	b_3^4	b_4^3	c_4^3	a_3^4
$\mathbf{O}_h(/\mathbf{D}_3)$	b_1^8	b_2^4	$b_1^4b_2^2$	c_2^4	c_2^4	c_2^4	$b_1^2b_3^2$	b_4^2	c_4^2	c_2c_6
$\mathbf{O}_h(/\mathbf{C}_{3v})$	b_1^8	b_2^4	b_2^4	c_2^4	$a_1^4c_2^2$	c_2^4	$b_1^2b_3^2$	b_4^2	c_4^2	c_2c_6
$\mathbf{O}_h(/\mathbf{D}_4)$	b_1^6	b_1^6	$b_1^2b_2^2$	c_2^3	c_2^3	c_2^3	b_3^2	$b_1^2b_2^2$	c_2^3	c_6
$\mathbf{O}_h(/\mathbf{C}_{4v})$	b_1^6	$b_1^2b_2^2$	b_2^3	$a_1^4c_2$	$a_1^2c_2^2$	c_2^3	b_3^2	$b_1^2b_4$	c_2c_4	c_6
$\mathbf{O}_h(/\mathbf{C}_{4h})$	b_1^6	$b_1^2b_2^2$	b_2^3	$a_1^2c_2^2$	c_2^3	a_1^6	b_3^2	$b_1^2b_4$	$a_1^2c_4$	a_3^2
$\mathbf{O}_h(/\mathbf{D}_{2d})$	b_1^6	b_1^6	b_2^3	c_2^3	$a_1^2c_2^2$	c_2^3	b_3^2	b_2^3	$a_1^2c_2^2$	c_6
$\mathbf{O}_h(/\mathbf{D}'_{2d})$	b_1^6	$b_1^2b_2^2$	$b_1^2b_2^2$	$a_1^4c_2$	c_2^3	c_2^3	b_3^2	b_2b_4	$a_1^2c_4$	c_6
$\mathbf{O}_h(/\mathbf{D}_{2h})$	b_1^6	b_1^6	b_2^3	a_1^6	c_2^3	a_1^6	b_3^2	b_2^3	c_2^3	a_3^2
$\mathbf{O}_h(/\mathbf{D}'_{2h})$	b_1^6	$b_1^2b_2^2$	$b_1^2b_2^2$	$a_1^2c_2^2$	$a_1^2c_2^2$	a_1^6	b_3^2	b_2b_4	c_2c_4	a_3^2
$\mathbf{O}_h(/\mathbf{T})$	b_1^4	b_1^4	b_2^2	c_2^2	c_2^2	c_2^2	b_1^4	b_2^2	c_2^2	c_2^2
$\mathbf{O}_h(/\mathbf{D}_{3d})$	b_1^4	b_2^2	$b_1^2b_2$	c_2^2	$a_1^2c_2$	a_1^4	b_1b_3	b_4	c_4	a_1a_3
$\mathbf{O}_h(/\mathbf{D}_{4h})$	b_1^3	b_1^3	b_1b_2	a_1^3	a_1c_2	a_1^3	b_3	b_1b_2	a_1c_2	a_3
$\mathbf{O}_h(/\mathbf{O})$	b_1^2	b_1^2	b_1^2	c_2	c_2	c_2	b_1^2	b_1^2	c_2	c_2
$\mathbf{O}_h(/\mathbf{T}_h)$	b_1^2	b_1^2	b_2	a_1^2	c_2	a_1^2	b_1^2	b_2	c_2	a_1^2
$\mathbf{O}_h(/\mathbf{T}_d)$	b_1^2	b_1^2	b_2	c_2	a_1^2	c_2	b_1^2	b_2	a_1^2	c_2
$\mathbf{O}_h(/\mathbf{O}_h)$	b_1	b_1	b_1	a_1	a_1	a_1	b_1	b_1	a_1	a_1
Σ	$\frac{1}{48}$	$\frac{1}{16}$	$\frac{1}{8}$	$\frac{1}{16}$	$\frac{1}{8}$	$\frac{1}{48}$	$\frac{1}{6}$	$\frac{1}{8}$	$\frac{1}{8}$	$\frac{1}{6}$

is shown in Appendix, was used for calculation. After the file was stored in a working directory named "c:/fujita0/", the following commands were input from the display of the Maple system:

```
>restart;
>read "c:/fujita0/markarac04.mpl";
```

The USCI-CF shown in Eq. 17 can be alternatively obtained by multiplying the multiplicity vector of Eq. 14 and the subduction-multiplicity matrix shown in the right-hand side of Eq. 6 as

follows:

$$(-\frac{1}{2},0,0,0,1,0,\frac{1}{2},0,0,0)\begin{array}{c}\\ \mathbf{O}_h(/\mathbf{C}_1)\downarrow\mathbf{S}_4\\ \mathbf{O}_h(/\mathbf{C}_2)\downarrow\mathbf{S}_4\\ \mathbf{O}_h(/\mathbf{C}'_2)\downarrow\mathbf{S}_4\\ \mathbf{O}_h(/\mathbf{C}_s)\downarrow\mathbf{S}_4\\ \mathbf{O}_h(/\mathbf{C}'_s)\downarrow\mathbf{S}_4\\ \mathbf{O}_h(/\mathbf{C}_i)\downarrow\mathbf{S}_4\\ \mathbf{O}_h(/\mathbf{C}_3)\downarrow\mathbf{S}_4\\ \mathbf{O}_h(/\mathbf{C}_4)\downarrow\mathbf{S}_4\\ \mathbf{O}_h(/\mathbf{S}_4)\downarrow\mathbf{S}_4\\ \mathbf{O}_h(/\mathbf{C}_{3i})\downarrow\mathbf{S}_4\end{array}\begin{array}{c}\begin{array}{ccc}\mathbf{C}_1 & \mathbf{C}_2 & \mathbf{S}_4\end{array}\\ \begin{pmatrix}12&0&0\\4&4&0\\6&0&0\\6&0&0\\6&0&0\\6&0&0\\4&0&0\\2&2&0\\2&0&4\\2&0&0\end{pmatrix}\end{array}=(2,0,0). \tag{18}$$

The resulting vector corresponds to $2\mathbf{S}_4(/\mathbf{C}_1)$. Because the $\mathbf{S}_4(/\mathbf{C}_1)$ is enantiospheric as well as $|\mathbf{S}_4|=4$ and $|\mathbf{C}_1|=1$, Eq. 18 results in a USCI-CF c_4^2, which is equal to Eq. 17.

The result of Eq. 18 is rationalized by considering the respective vectors contained in the matrix of the right-hand side. Note that the vector $(12,0,0)$ for $\mathbf{O}_h(/\mathbf{C}_1)\downarrow\mathbf{S}_4$ means $12\mathbf{S}_4(/\mathbf{C}_1)$, the vector $(6,0,0)$ for $\mathbf{O}_h(/\mathbf{C}'_s)\downarrow\mathbf{S}_4$ means $6\mathbf{S}_4(/\mathbf{C}_1)$, and the vector $(4,0,0)$ for $\mathbf{O}_h(/\mathbf{C}_3)\downarrow\mathbf{S}_4$ means $4\mathbf{S}_4(/\mathbf{C}_1)$. Hence, the multiplicity vector appearing in the left-hand side of Eq. 18 indicates:

$$-\frac{1}{2}\times 12\mathbf{S}_4(/\mathbf{C}_1)+1\times 6\mathbf{S}_4(/\mathbf{C}_1)+\frac{1}{2}\times 4\mathbf{S}_4(/\mathbf{C}_1)=2\mathbf{S}_4(/\mathbf{C}_1), \tag{19}$$

which corresponds to the vector of Eq. 18.

Via Direct Subductions The procedure for the subductions of dominant representations (e.g., Eq. 6 for $\mathbf{O}_h$) can be also applied to non-dominant representations according to Subsection 3.2 of [27]. This provides us with an alternative method of calculating USCI-CFs for non-dominant representations. For example, several markaracters listed in the left part of Table 4 are subduced into $\mathbf{S}_4$ (i.e., by selecting the values corresponding to $\mathbf{C}_1$, $\mathbf{C}_2$, and $\mathbf{S}_4$) and multiplied by the inverse ($\widetilde{\mathrm{M}}_{\mathbf{S}_4}^{-1}$) so as to give the following result:

$$\begin{array}{c}\\ \mathbf{O}_h(/\mathbf{D}_2)\\ \mathbf{O}_h(/\mathbf{D}'_2)\\ \mathbf{O}_h(/\mathbf{C}_{2v})\\ \mathbf{O}_h(/\mathbf{C}'_{2v})\\ \mathbf{O}_h(/\mathbf{C}''_{2v})\\ \mathbf{O}_h(/\mathbf{C}_{2h})\\ \mathbf{O}_h(/\mathbf{C}'_{2h})\\ \mathbf{O}_h(/\mathbf{D}_3)\\ \mathbf{O}_h(/\mathbf{C}_{3v})\\ \mathbf{O}_h(/\mathbf{D}_4)\\ \mathbf{O}_h(/\mathbf{C}_{4v})\end{array}\begin{array}{c}\begin{array}{ccc}\mathbf{C}_1 & \mathbf{C}_2 & \mathbf{S}_4\end{array}\\ \begin{pmatrix}12&12&0\\12&4&0\\12&4&0\\12&4&0\\12&0&0\\12&4&0\\12&0&0\\8&0&0\\8&0&0\\6&6&0\\6&2&0\end{pmatrix}\end{array}\begin{pmatrix}\frac{1}{4}&0&0\\-\frac{1}{4}&\frac{1}{2}&0\\0&-\frac{1}{2}&1\end{pmatrix}=\begin{array}{c}\\ \mathbf{O}_h(/\mathbf{D}_2)\downarrow\mathbf{S}_4\\ \mathbf{O}_h(/\mathbf{D}'_2)\downarrow\mathbf{S}_4\\ \mathbf{O}_h(/\mathbf{C}_{2v})\downarrow\mathbf{S}_4\\ \mathbf{O}_h(/\mathbf{C}'_{2v})\downarrow\mathbf{S}_4\\ \mathbf{O}_h(/\mathbf{C}''_{2v})\downarrow\mathbf{S}_4\\ \mathbf{O}_h(/\mathbf{C}_{2h})\downarrow\mathbf{S}_4\\ \mathbf{O}_h(/\mathbf{C}'_{2h})\downarrow\mathbf{S}_4\\ \mathbf{O}_h(/\mathbf{D}_3)\downarrow\mathbf{S}_4\\ \mathbf{O}_h(/\mathbf{C}_{3v})\downarrow\mathbf{S}_4\\ \mathbf{O}_h(/\mathbf{D}_4)\downarrow\mathbf{S}_4\\ \mathbf{O}_h(/\mathbf{C}_{4v})\downarrow\mathbf{S}_4\end{array}\begin{array}{c}\begin{array}{ccc}\mathbf{C}_1 & \mathbf{C}_2 & \mathbf{S}_4\end{array}\\ \begin{pmatrix}0&6&0\\2&2&0\\2&2&0\\2&2&0\\3&0&0\\2&2&0\\3&0&0\\2&0&0\\2&0&0\\0&3&0\\1&1&0\end{pmatrix}\end{array}\begin{array}{c}\\ c_2^6\\ c_2^2c_4^2\\ c_2^2c_4^2\\ c_2^2c_4^2\\ c_4^3\\ c_2^2c_4^2\\ c_4^3\\ c_4^2\\ c_4^2\\ c_2^3\\ c_2c_4\end{array}. \tag{20}$$

The $\mathbf{O}_h(/\mathbf{C}_{3v})\downarrow\mathbf{S}_4$-row in the matrix of the right-hand side of Eq. 20 is identical with the vector of Eq. 18, which corresponds to $2\mathbf{S}_4(/\mathbf{C}_1)$. The corresponding USCI-CF c_4^2 is collected along with the other USCI-CFs in the rightmost part of Eq. 20. These USCI-CFs have appeared as part of the $\mathbf{S}_4$-column in Table 5.

3 Tables for the Point Group O

3.1 Mark Table, Inverse Mark Table, and USCI-CF Table of O

From the elements of $\mathbf{O}_h$ collected in Eq. 1, all of the proper rotations are selected to give the point group $\mathbf{O}$ of order 24:

$$\begin{aligned}\mathbf{O} \;=\; \Big\{ & I, C_{2(1)}, C_{2(2)}, C_{2(3)}; C_{3(1)}, C_{3(3)}, C_{3(2)}, C_{3(4)}, C^2_{3(1)}, C^2_{3(4)}, C^2_{3(3)}, C^2_{3(2)}, \\ & C'_{2(6)}, C'_{2(1)}, C'_{2(4)}, C'_{2(2)}, C'_{2(5)}, C'_{2(3)}, C^3_{4(3)}, C_{4(3)}, C^3_{4(1)}, C_{4(1)}, C_{4(2)}, C^3_{4(2)} \Big\}. \end{aligned} \tag{21}$$

The point group $\mathbf{O}$ has 11 subgroups up to conjugacy, which is selected as a non-redundant set of subgroups (SSG):

$$\mathrm{SSG}_{\mathbf{O}} = \left\{ \mathbf{C}_1, \mathbf{C}_2, \mathbf{C}'_2, \mathbf{C}_3, \mathbf{C}_4, \mathbf{D}_2, \mathbf{D}'_2, \mathbf{D}_3, \mathbf{D}_4, \mathbf{T}, \mathbf{O} \right\}, \tag{22}$$

where the subgroups are aligned in the ascending order of their orders. The respective subgroups correspond to the coset representations $\mathbf{O}(/\mathbf{G}_i)$ ($\mathbf{G}_i \in \mathrm{SSG}_{\mathbf{O}}$) according to the formulation of the USCI approach [21]. The coset representations are characterized by their marks as collected in respective rows of the mark table of $\mathbf{O}$, as shown in Table 6. The inverse of the mark table of $\mathbf{O}$ is shown in Table 7. Because the $\mathbf{O}$ group is isomorphic with the point group $\mathbf{T}_d$, Tables 6 and 7 contain the same values as found in the respective counterparts of $\mathbf{T}_d$, i.e., the mark table of $\mathbf{T}_d$ (Table A.10 of Appendix A in [21]) and its inverse (Table B.10 of Appendix B in [21]).

On the other hand, the USCI-CF table of $\mathbf{O}$ (Table 8), which has been obtained according to Chapter 9 of [21], is different from the counterpart of of $\mathbf{T}_d$ shown in Table E.10 of Appendix E of [21], because the sphericity of each SI is hemispheric to be b_d for $\mathbf{O}$. For example, the subduction $\mathbf{O}(/\mathbf{T}) \downarrow \mathbf{C}_4$ corresponds to $\mathbf{C}_4(/\mathbf{C}_2)$ (hemispheric) so as to give a USCI-CF b_2, while the corresponding subduction $\mathbf{T}_d(/\mathbf{T}) \downarrow \mathbf{S}_4$ corresponds to $\mathbf{S}_4(/\mathbf{C}_2)$ (enantiospheric) so as to give a USCI-CF c_2 (note that the USCI-CF a_2 of Table E.10 of Appendix E in [21] is erroneous and should be corrected).

3.2 Considering Cyclic Subgroups of O

3.2.1 Markaracter Table and Inverse Markaracter Table of O

By selecting cyclic subgroups from the subgroups shown in Eq. 21 according to [26], we obtain a non-redundant set of cyclic subgroups (SCSG) as follows:

$$\mathrm{SCSG}_{\mathbf{O}} = \left\{ \mathbf{C}_1, \mathbf{C}_2, \mathbf{C}'_2, \mathbf{C}_3, \mathbf{C}_4 \right\}. \tag{23}$$

The respective subgroups correspond to the coset representations $\mathbf{O}(/\mathbf{G}_i)$ ($\mathbf{G}_i \in \mathrm{SCSG}_{\mathbf{O}}$) called *dominant representations*, which can be restricted to a set of elements corresponding to $\mathrm{SCSG}_{\mathbf{O}}$. They are collected to give the markaracter table of $\mathbf{O}$ (Table 9). The task of generating such a markaracter table can be illustrated by the conversion of a mark table into a modified mark table, where the elements for cyclic subgroups are collected in the upper left part [26]. Fortunately, the mark table of $\mathbf{O}$ shown in Table 6 can be regarded as a modified mark table as it is. The resulting upper left part of the modified mark table (divided by a horizontal and a vertical line) indicates the corresponding markaracter table, which is shown separately in Table 9. Similarly, the inverse (Table 7) is regarded as a modified form, from which the upper left part is separated to give the corresponding inverse of the markaracter table (Table 10).

Table 6: (Modified) Mark Table of $\mathbf{O}$

$M_{\mathbf{O}}$	$\mathbf{C}_1$	$\mathbf{C}_2$	$\mathbf{C}_2'$	$\mathbf{C}_3$	$\mathbf{C}_4$	$\mathbf{D}_2$	$\mathbf{D}_2'$	$\mathbf{D}_3$	$\mathbf{D}_4$	$\mathbf{T}$	$\mathbf{O}$
$\mathbf{O}(/\mathbf{C}_1)$	24	0	0	0	0	0	0	0	0	0	0
$\mathbf{O}(/\mathbf{C}_2)$	12	4	0	0	0	0	0	0	0	0	0
$\mathbf{O}(/\mathbf{C}_2')$	12	0	2	0	0	0	0	0	0	0	0
$\mathbf{O}(/\mathbf{C}_3)$	8	0	0	2	0	0	0	0	0	0	0
$\mathbf{O}(/\mathbf{C}_4)$	6	2	0	0	2	0	0	0	0	0	0
$\mathbf{O}(/\mathbf{D}_2)$	6	6	0	0	0	6	0	0	0	0	0
$\mathbf{O}(/\mathbf{D}_2')$	6	2	2	0	0	0	2	0	0	0	0
$\mathbf{O}(/\mathbf{D}_3)$	4	0	2	1	0	0	0	1	0	0	0
$\mathbf{O}(/\mathbf{D}_4)$	3	3	1	0	1	3	1	0	1	0	0
$\mathbf{O}(/\mathbf{T})$	2	2	0	2	0	2	0	0	0	2	0
$\mathbf{O}(/\mathbf{O})$	1	1	1	1	1	1	1	1	1	1	1

Table 7: (Modified) Inverse Mark Table of $\mathbf{O}$

$M_{\mathbf{O}}^{-1}$	$\mathbf{O}$ $(/\mathbf{C}_1)$	$\mathbf{O}$ $(/\mathbf{C}_2)$	$\mathbf{O}$ $(/\mathbf{C}_2')$	$\mathbf{O}$ $(/\mathbf{C}_3)$	$\mathbf{O}$ $(/\mathbf{C}_4)$	$\mathbf{O}$ $(/\mathbf{D}_2)$	$\mathbf{O}$ $(/\mathbf{D}_2')$	$\mathbf{O}$ $(/\mathbf{D}_3)$	$\mathbf{O}$ $(/\mathbf{D}_4)$	$\mathbf{O}$ $(/\mathbf{T})$	$\mathbf{O}$ $(/\mathbf{O})$	Σ
$\mathbf{C}_1$	$\frac{1}{24}$	0	0	0	0	0	0	0	0	0	0	$\frac{1}{24}$
$\mathbf{C}_2$	$-\frac{1}{8}$	$\frac{1}{4}$	0	0	0	0	0	0	0	0	0	$\frac{1}{8}$
$\mathbf{C}_2'$	$-\frac{1}{4}$	0	$\frac{1}{2}$	0	0	0	0	0	0	0	0	$\frac{1}{4}$
$\mathbf{C}_3$	$-\frac{1}{6}$	0	0	$\frac{1}{2}$	0	0	0	0	0	0	0	$\frac{1}{3}$
$\mathbf{C}_4$	0	$-\frac{1}{4}$	0	0	$\frac{1}{2}$	0	0	0	0	0	0	$\frac{1}{4}$
$\mathbf{D}_2$	$\frac{1}{12}$	$-\frac{1}{4}$	0	0	0	$\frac{1}{6}$	0	0	0	0	0	0
$\mathbf{D}_2'$	$\frac{1}{4}$	$-\frac{1}{4}$	$-\frac{1}{2}$	0	0	0	$\frac{1}{2}$	0	0	0	0	0
$\mathbf{D}_3$	$\frac{1}{2}$	0	-1	$-\frac{1}{2}$	0	0	0	1	0	0	0	0
$\mathbf{D}_4$	0	$\frac{1}{2}$	0	0	$-\frac{1}{2}$	$-\frac{1}{2}$	$-\frac{1}{2}$	0	1	0	0	0
$\mathbf{T}$	$\frac{1}{6}$	0	0	$-\frac{1}{2}$	0	$-\frac{1}{6}$	0	0	0	$\frac{1}{2}$	0	0
$\mathbf{O}$	$-\frac{1}{2}$	0	1	$\frac{1}{2}$	0	$\frac{1}{2}$	0	-1	-1	$-\frac{1}{2}$	1	0

Table 8: USCI-CF Table of **O**

	$\mathbf{C}_1$	$\mathbf{C}_2$	$\mathbf{C}_2'$	$\mathbf{C}_3$	$\mathbf{C}_4$	$\mathbf{D}_2$	$\mathbf{D}_2'$	$\mathbf{D}_3$	$\mathbf{D}_4$	$\mathbf{T}$	$\mathbf{O}$
$\mathbf{O}(/\mathbf{C}_1)$	b_1^{24}	b_2^{12}	b_2^{12}	b_3^8	b_4^6	b_4^6	b_4^6	b_6^4	b_8^3	b_{12}^2	b_{24}
$\mathbf{O}(/\mathbf{C}_2)$	b_1^{12}	$b_1^4b_2^4$	b_2^6	b_3^4	$b_2^2b_4^2$	b_2^6	$b_2^2b_4^2$	b_6^2	b_4^3	b_6^2	b_{12}
$\mathbf{O}(/\mathbf{C}_2')$	b_1^{12}	b_2^6	$b_1^2b_2^5$	b_3^4	b_4^3	b_4^3	$b_2^2b_4^2$	$b_3^2b_6$	b_4b_8	b_{12}	b_{12}
$\mathbf{O}(/\mathbf{C}_3)$	b_1^8	b_2^4	b_2^4	$b_1^2b_3^2$	b_4^2	b_4^2	b_4^2	b_2b_6	b_8	b_4^2	b_8
$\mathbf{O}(/\mathbf{C}_4)$	b_1^6	$b_1^2b_2^2$	b_2^3	b_3^2	$b_1^2b_4$	b_2^3	b_2b_4	b_6	b_2b_4	b_6	b_6
$\mathbf{O}(/\mathbf{D}_2)$	b_1^6	b_1^6	b_2^3	b_3^2	b_2^3	b_1^6	b_2^3	b_6	b_2^3	b_3^2	b_6
$\mathbf{O}(/\mathbf{D}_2')$	b_1^6	$b_1^2b_2^2$	$b_1^2b_2^2$	b_3^2	b_2b_4	b_2^3	$b_1^2b_4$	b_3^2	b_2b_4	b_6	b_6
$\mathbf{O}(/\mathbf{D}_3)$	b_1^4	b_2^2	$b_1^2b_2$	b_1b_3	b_4	b_4	b_2^2	b_1b_3	b_4	b_4	b_4
$\mathbf{O}(/\mathbf{D}_4)$	b_1^3	b_1^3	b_1b_2	b_3	b_1b_2	b_1^3	b_1b_2	b_3	b_1b_2	b_3	b_3
$\mathbf{O}(/\mathbf{T})$	b_1^2	b_1^2	b_2	b_1^2	b_2	b_1^2	b_2	b_2	b_2	b_1^2	b_2
$\mathbf{O}(/\mathbf{O})$	b_1	b_1	b_1	b_1	b_1	b_1	b_1	b_1	b_1	b_1	b_1
$\sum$	1/24	1/8	1/4	1/3	1/4	0	0	0	0	0	0

Table 9: Markaracter Table of **O**

$\widetilde{\mathrm{M}}_{\mathbf{O}}$	$\mathbf{C}_1$	$\mathbf{C}_2$	$\mathbf{C}_2'$	$\mathbf{C}_3$	$\mathbf{C}_4$
$\mathbf{O}(/\mathbf{C}_1)$	24	0	0	0	0
$\mathbf{O}(/\mathbf{C}_2)$	12	4	0	0	0
$\mathbf{O}(/\mathbf{C}_2')$	12	0	2	0	0
$\mathbf{O}(/\mathbf{C}_3)$	8	0	0	2	0
$\mathbf{O}(/\mathbf{C}_4)$	6	2	0	0	2

Table 10: Inverse Markaracter Table of **O**

$\widetilde{\mathrm{M}}_{\mathbf{O}}^{-1}$	$\mathbf{O}$ $(/\mathbf{C}_1)$	$\mathbf{O}$ $(/\mathbf{C}_2)$	$\mathbf{O}$ $(/\mathbf{C}_2')$	$\mathbf{O}$ $(/\mathbf{C}_3)$	$\mathbf{O}$ $(/\mathbf{C}_4)$	Σ
$\mathbf{C}_1$	$\frac{1}{24}$	0	0	0	0	$\frac{1}{24}$
$\mathbf{C}_2$	$-\frac{1}{8}$	$\frac{1}{4}$	0	0	0	$\frac{1}{8}$
$\mathbf{C}_2'$	$-\frac{1}{4}$	0	$\frac{1}{2}$	0	0	$\frac{1}{4}$
$\mathbf{C}_3$	$-\frac{1}{6}$	0	0	$\frac{1}{2}$	0	$\frac{1}{3}$
$\mathbf{C}_4$	0	$-\frac{1}{4}$	0	0	$\frac{1}{2}$	$\frac{1}{4}$

3.2.2 Dominant USCI-CF Table of O

On a similar line to 2.1.3 (e.g., Eq. 6), a part of Table 9 specified for a given cyclic subgroup is selected to generate a subduced markaracter, which is multiplied by the inverse of the markaracter of the cyclic subgroup so as to give the corresponding subduction-multiplicity matrix. The resulting matrix generates a set of products of SIs in a similar way to the rightmost part of Eq. 6. This procedure is repeated for every cyclic subgroups so as to give the data for a dominant USCI-CF table, e.g., Table 11 of the present case. Because the point group **O** is isomorphic with the point group $\mathbf{T}_d$, the dominant USCI table of $\mathbf{T}_d$, which has been obtained by this procedure [26, 28], can be converted into the dominant USCI-CF table of **O** by substituting the SI b_d for s_d.

Table 11: Dominant USCI-CF Table of **O**

	$\mathbf{C}_1$	$\mathbf{C}_2$	$\mathbf{C}'_2$	$\mathbf{C}_3$	$\mathbf{C}_4$
O(/$\mathbf{C}_1$)	b_1^{24}	b_2^{12}	b_2^{12}	b_3^8	b_4^6
O(/$\mathbf{C}_2$)	b_1^{12}	$b_1^4b_2^4$	b_2^6	b_3^4	$b_2^2b_4^2$
O(/$\mathbf{C}'_2$)	b_1^{12}	b_2^6	$b_1^2b_2^5$	b_3^4	b_4^3
O(/$\mathbf{C}_3$)	b_1^8	b_2^4	b_2^4	$b_1^2b_3^2$	b_4^2
O(/$\mathbf{C}_4$)	b_1^6	$b_1^2b_2^2$	b_2^3	b_3^2	$b_1^2b_4$
$\sum$	1/24	1/8	1/4	1/3	1/4

Table 12: Non-Dominant USCI-CF Table of **O**

	$\mathbf{C}_1$	$\mathbf{C}_2$	$\mathbf{C}'_2$	$\mathbf{C}_3$	$\mathbf{C}_4$
O(/$\mathbf{D}_2$)	b_1^6	b_1^6	b_2^3	b_3^2	b_2^3
O(/$\mathbf{D}'_2$)	b_1^6	$b_1^2b_2^2$	$b_1^2b_2^2$	b_3^2	b_2b_4
O(/$\mathbf{D}_3$)	b_1^4	b_2^2	$b_1^2b_2$	b_1b_3	b_4
O(/$\mathbf{D}_4$)	b_1^3	b_1^3	b_1b_2	b_3	b_1b_2
O(/**T**)	b_1^2	b_1^2	b_2	b_1^2	b_2
O(/**O**)	b_1	b_1	b_1	b_1	b_1
$\sum$	1/24	1/8	1/4	1/3	1/4

Alternatively, the dominant USCI-CF Table (e.g., Table 11) appears in the corresponding USCI-CF Table (e.g., Table 8), as illustrated in the upper left part of Table 8.

3.2.3 Non-Dominant USCI-CF Table of O

Via Multiplicity Vectors Each row of Table 6, $\widetilde{\mathrm{M}}_{\mathbf{O}(/\mathbf{G}_i)}$ ($\mathbf{G}_i \notin \mathrm{SCSG}_{\mathbf{O}}$), other than the dominant representations is multiplied by the inverse $\widetilde{\mathrm{M}}_{\mathbf{O}}^{-1}$ (Table 10) to give a multiplicity vector. The resulting multiplicity vector is capable of calculating USCIs (or USCI-CFs) for non-dominant representations according to Theorem 4 of [27]. In a similar way to the case described

for $\mathbf{O}_h$, a maple program akin to the one listed in Appendix is written to obtain the full data of Table 12 by starting from the dominant USCI-CF table (Table 11).

Obviously, the non-dominant USCI-CF table of $\mathbf{O}$ (Table 12) is contained as a part of the USCI-CF table of $\mathbf{O}$ (Table 8).

Via Direct Subductions Each row of Table 6 other than the dominant representations, i.e., $\widetilde{\mathrm{M}}_{\mathbf{O}(/\mathbf{G}_i)}$ ($\mathbf{G}_i \notin \mathrm{SCSG}_{\mathbf{O}}$), is also subduced into a cyclic subgroup $\mathbf{G}_j$. The resulting vector is multiplied by the inverse $\widetilde{\mathrm{M}}^{-1}_{\mathbf{G}_j}$ (e.g., for the $\mathbf{S}_4$ shown in Eq. 20) on a similar line to Eq. 20. The resulting USCI-CFs are collected to give Table 12.

4 Enumeration Based on the Markaracter Method

The markaracter method proposed by us [26, 27] uses the concept of markaracters and related concepts such as markaracter tables, their inverse, dominant USCI tables, multiplicity vectors, and so on. Because these concepts were formulated without considering chirality fittingness [26, 27], they have been extended into more general concepts with chirality fittingness, e.g., dominant USCIs into dominant USCI-CFs, by using the point groups $\mathbf{O}_h$ and $\mathbf{O}$ as examples in the preceding sections. In this section, we first extend the previous formulation of the enumeration procedure (without chirality fittingness) adopted in the markaracter method [26, 27] into a more general version with chirality fittingness. Then, the extended version is applied to enumeration of cubanes of the $\mathbf{O}_h$-symmetry.

4.1 Subduced Cycle Indices via Multiplicity Vectors

In combinatorial enumeration based on the USCI approach [21], such a non-dominant USCI-CF as collected in Table 5 can be regarded as referring to a single orbit governed by a coset representation $\mathbf{G}(/\mathbf{G}_i)$ (e.g., $\mathbf{O}_h(/\mathbf{G}_i)$ for $\mathbf{G}_i \in \mathrm{SSG}_{\mathbf{O}_h}$ and $\mathbf{G}_i \notin \mathrm{SCSG}_{\mathbf{O}_h}$). In other words, the non-dominant USCI-CF can be in turn regarded as a subduced cycle index with chirality fittingness (SCI-CF) for such a single orbit. As found by a careful examination, the method of preparing non-dominant USCI-CFs (described in 2.2.2) can be applied to generate SCI-CF for cases having two or more orbits (two or more coset representations), where a vector of markaracters is a sum of vectors of markaracters at issue. It should be noted that the present SCI-CFs are concerned with monomials for the SCSG (cf. Table 11), while the SCI-CFs defined generally in the USCI approach [21] are concerned with monomials for the SSG (cf. Table 8). They are not differentiated so long as such usage causes no confusion.

Suppose that a given markaracter $\widetilde{\mathrm{M}}_{\mathbf{P}}$ is concerned with a permutation representation $\mathbf{P}$ of the point group $\mathbf{G}$:

$$\widetilde{\mathrm{M}}_{\mathbf{P}} = (\delta_1, \delta_2, \ldots, \delta_s), \tag{24}$$

where δ_i denotes the number of fixed objects of $\mathbf{P}$ on the action of the cyclic subgroup $\mathbf{G}_i$ ($\in \mathrm{SCSG}_{\mathbf{G}}$). The markaracter $\widetilde{\mathrm{M}}_{\mathbf{P}}$ is regarded as a vector, which is multiplied by the inverse markaracter table of the group $\mathbf{G}$, i.e., $\widetilde{\mathrm{M}}^{-1}_{\mathbf{G}}$ ($= (\overline{m}_{ji})$), so as to generate a multiplicity vector, $\widetilde{\mathrm{A}}$:

$$\widetilde{\mathrm{A}} = \widetilde{\mathrm{M}}_{\mathbf{P}}\widetilde{\mathrm{M}}^{-1}_{\mathbf{G}} = (\widetilde{\alpha}_1, \widetilde{\alpha}_2, \ldots, \widetilde{\alpha}_s), \tag{25}$$

which corresponds to the following sum of coset representations:

$$\mathbf{P} = \sum_{i=1}^{s} \widetilde{\alpha}_s \mathbf{G}(/\mathbf{G}_i), \tag{26}$$

where $\mathbf{G}_i \in \mathrm{SCSG}_{\mathbf{G}}$.

By referring to the subduction (Eq. 10) and the corresponding USCI-CF (Eq. 11), the formulation described in Subsection of 3.3 of [27] is extended by considering chirality fittingness so as to give the following subduced cycle index with chirality fittingness (SCI-CF):

$$\begin{aligned} \text{SCI-CF}(\mathbf{P} \downarrow \mathbf{G}_j; \$_{d_{jk}}) &= \prod_{i=1}^{s} \left(\mathrm{Z}(\mathbf{G}(/\mathbf{G}_i) \downarrow \mathbf{G}_j; \$_{d_{jk}}) \right)^{\widetilde{\alpha}_i} \\ &= \prod_{i=1}^{s} \left(\prod_{k=1}^{r_j} \$_{d_{jk}}^{\beta_k^{(ij)}} \right)^{\widetilde{\alpha}_i} = \prod_{k=1}^{r_j} \$_{d_{jk}}^{\beta_k^{(j)}}, \end{aligned} \tag{27}$$

where $\mathbf{P} \downarrow \mathbf{G}_j$ ($j = 1, 2, \ldots, s$) represents a sum of $\mathbf{G}(/\mathbf{G}_i) \downarrow \mathbf{G}_j$ (corresponding to Eq. 26) and

$$\beta_k^{(j)} = \sum_{i=1}^{s} \widetilde{\alpha}_i \beta_k^{(ij)}. \tag{28}$$

In general, SCI-CFs are calculated by using Eq. 27, where such a Maple program as listed in Appendix can be also used. For example, suppose that a vector of markaracters is given to be $(14,2,0,4,6,0,2,2,0,0)$, which is the sum of the $\widetilde{\mathrm{M}}_{\mathbf{O}_h(/\mathbf{C}_{3v})}$- and $\widetilde{\mathrm{M}}_{\mathbf{O}_h(/\mathbf{C}_{4v})}$-rows of Table 4. Then, the following line:

```
m:= vector([14,2,0,4,6,0,2,2,0,0]); ndUSCIcf(m);
```

is added at the last of the Maple program listed in Appendix. Thereby, we obtain the following SCI-CF for this case:

$$\text{SCI-CF} = (b_1^{14}, b_1^2 b_2^6, b_2^7, a_1^4 c_2^5, a_1^6 c_2^4, c_2^7, b_1^2 b_3^4, b_1^2 b_4^3, c_2 c_4^3, c_2 c_6^2), \tag{29}$$

which is recognized to be calculated from the data of the dominant USCI-CF table (Table 3) via a multiplicity vector. Obviously, this SCI-CF is also obtained from the data of the $\mathbf{O}_h(/\mathbf{C}_{3v})$- and $\mathbf{O}_h(/\mathbf{C}_{3v})$-rows of Table 5.

4.2 Cycle Indices Based on Dominant USCI-CF Tables

The markaracter method formulated in Subsection 3.3 of [27] is concerned with dominant USCI tables without chirality fittingness. This treatment is here extended to provide the markaracter method with considering chirality fittingness in the light of the USCI approach [21].

Let a skeleton with n positions belong to a point group $\mathbf{G}$, which is characterized by the SCSG represented by Eq. 9. The n positions of the skeleton are governed by a permutation representation $\mathbf{P}$, which has a markaracter $\widetilde{\mathrm{M}}_{\mathbf{P}}$ (Eq. 24). The markaracter $\widetilde{\mathrm{M}}_{\mathbf{P}}$ is regarded as a vector, which is multiplied by the inverse markaracter table of the group $\mathbf{G}$, i.e., $\widetilde{\mathrm{M}}_{\mathbf{G}}^{-1}$ $(= (\overline{m}_{ji}))$ so as to generate the corresponding multiplicity vector $\widetilde{\mathrm{A}}$ (Eq. 25). Thereby, the corresponding SCI-CF is obtained as shown in Eq. 27. The formulation (Eq. 74) described in Subsection of 3.3

of [27] is extended by considering chirality fittingness so as to give the following cycle index with chirality fittingness (CI-CF):

$$\begin{aligned}
\text{CI-CF}(\mathbf{P};\$_{d_{jk}}) &= \sum_{j=1}^{s}\left(\left(\sum_{i=1}^{s}\overline{m}_{ji}\right)\text{SCI-CF}(\mathbf{P}\downarrow\mathbf{G}_j;\$_{d_{jk}})\right)\\
&= \sum_{j=1}^{s}\left(\left(\sum_{i=1}^{s}\overline{m}_{ji}\right)\prod_{i=1}^{s}\left(\text{Z}(\mathbf{G}(/\mathbf{G}_i)\downarrow\mathbf{G}_j;\$_{d_{jk}})\right)^{\widetilde{\alpha}_i}\right)\\
&= \sum_{j=1}^{s}\left(\left(\sum_{i=1}^{s}\overline{m}_{ji}\right)\prod_{i=1}^{s}\left(\prod_{k=1}^{r_j}\$_{d_{jk}}^{\beta_k^{(ij)}}\right)^{\widetilde{\alpha}_i}\right)\\
&= \sum_{j=1}^{s}\left(\left(\sum_{i=1}^{s}\overline{m}_{ji}\right)\prod_{k=1}^{r_j}\$_{d_{jk}}^{\beta_k^{(j)}}\right), \qquad (30)
\end{aligned}$$

where

$$\beta_k^{(j)} = \sum_{i=1}^{s}\widetilde{\alpha}_i\beta_k^{(ij)}. \qquad (31)$$

Note that the summation of $\sum_{i=1}^{s}\overline{m}_{ji}$ represents the sum of each $\mathbf{G}_j$-row (cf. the rightmost $\sum$-column of Table 2).

It should be noted here that the CI-CF shown in Eq. 30 is identical with Def. 19.7 of [21], because the monomials concerning non-cyclic subgroups vanish in the previous formulation for Def. 19.7 of [21].

On the basis of the CI-CF shown in Eq. 30, Theorem 5 of [27], which is concerned with a CI without chirality fittingness, can be extended to take account of chirality fittingness as follows:

Theorem 1 Suppose that the n positions of the above skeleton belonging to a point group $\mathbf{G}$ accommodate n proligands selected from the following proligand inventory:

$$\mathbf{X} = \{\mathrm{x}_1,\mathrm{x}_2,\ldots,\mathrm{x}_v;\mathrm{p}_1,\mathrm{p}_2,\ldots\mathrm{p}_v;\overline{\mathrm{p}}_1,\overline{\mathrm{p}}_2,\ldots,\overline{\mathrm{p}}_v\} \qquad (32)$$

where each x_ℓ represents an achiral proligand and each pair of p_ℓ and $\overline{\mathrm{p}}_\ell$ represents an enantiomeric pair of chiral proligands. Consider isomers having θ_ℓ of x_ℓ, θ'_ℓ of p_ℓ, and θ''_ℓ of $\overline{\mathrm{p}}_\ell$, which are characterized by the formula:

$$W_\theta = \prod_{\ell=1}^{v}\mathrm{x}_\ell^{\theta_\ell}\prod_{\ell=1}^{v}\mathrm{p}_\ell^{\theta'_\ell}\prod_{\ell=1}^{v}\overline{\mathrm{p}}_\ell^{\theta''_\ell}, \qquad (33)$$

where $[\theta]$ represents a partition:

$$[\theta]:\sum_{\ell=1}^{v}\theta_\ell+\sum_{\ell=1}^{v}\theta'_\ell+\sum_{\ell=1}^{v}\theta''_\ell = n. \qquad (34)$$

Let the symbol A_θ denote the number of such isomers as having $[\theta]$. Then a generating function for the gross number of isomers is represented by:

$$\sum_{[\theta]}A_\theta W_\theta = \text{CI-CF}(\mathbf{P};\$_{d_{jk}}), \qquad (35)$$

where the CI-CF is represented by Eq. 30 and each $\$_{d_{jk}}$ ($a_{d_{jk}}$, $b_{d_{jk}}$, or $c_{d_{jk}}$) is substituted by either one of the following ligand-inventory functions:

$$a_{d_{jk}} = \sum_{\ell=1}^{v} \mathrm{x}_\ell^{d_{jk}} \tag{36}$$

$$b_{d_{jk}} = \sum_{\ell=1}^{v} \mathrm{x}_\ell^{d_{jk}} + \sum_{\ell=1}^{v} \mathrm{p}_\ell^{d_{jk}} + \sum_{\ell=1}^{v} \overline{\mathrm{p}}_\ell^{d_{jk}} \tag{37}$$

$$c_{d_{jk}} = \sum_{\ell=1}^{v} \mathrm{x}_\ell^{d_{jk}} + 2\sum_{\ell=1}^{v} \mathrm{p}_\ell^{d_{jk}/2}\overline{\mathrm{p}}_\ell^{d_{jk}/2}. \tag{38}$$

It should be noted here that Theorem 1 is equivalent to Theorem 1 of [32] (the proligand method), although they are different in the fact that the former theorem is concerned with conjugate cyclic subgroups, while the latter theorem is concerned with conjugacy classes.

4.3 Enumeration of Cubane Derivatives

4.3.1 Cubane Derivatives as Three-Dimensional Structural Isomers

The numbering of a cubane skeleton belonging to the $\mathbf{O}_h$-point group is shown in **1** (Figure 1). The 8 positions generates 48 permutations on the action of the 48 elements of $\mathbf{O}_h$ (Eq. 1), where

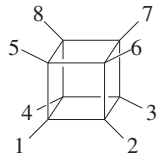

1

Figure 1: Numbering of the eight positions of cubane (**1**)

they construct a permutation representation **P**. The markaracter for characterizing **P** is obtained by counting fixed positions on the action of each cyclic subgroup. For example, let us examine the point group $\mathbf{C}_3 = \{I, C_{3(1)}, C_{3(1)}^2\}$, which is concerned with the three-fold axis through the positions 4 and 6 in the cubane skeleton (**1**). Permutations (as products of cycles) corresponding to the $\mathbf{C}_3$ group are selected from **P** as follows:

I	(1)(2)(3)(4)(5)(6)(7)(8)
$C_{3(1)}$	(4)(6)(1 8 3)(2 5 7)
$C_{3(1)}^2$	(4)(6)(1 3 8)(2 7 5)
fixed positions	(4) and (6)

Because two positions 4 and 6 are fixed as designated by one-cycles, the value 2 is placed as the $\mathbf{C}_3$-component of the markaracter $\widetilde{\mathrm{M}}_{\mathbf{P}}$. This procedure is repeated to cover all of the cyclic subgroups of the $\mathrm{SCSG}_{\mathbf{O}_h}$ (Eq. 3) so as to give the markaracter:

$$\widetilde{\mathrm{M}}_{\mathbf{P}} = (8,0,0,0,4,0,2,0,0,0), \tag{39}$$

which is identical with $\widetilde{\mathrm{M}}_{\mathbf{O}_h(/\mathbf{C}_{3v})}$ (Eq. 5). The corresponding multiplicity vector, which has been calculated as shown in the $\widetilde{\mathrm{M}}_{\mathbf{O}_h(/\mathbf{C}_{3v})}$-row of Table 4, is further applied to calculate the corresponding non-dominant USCI-CF (the $\mathbf{O}_h(/\mathbf{C}_{3v})$-row of Table 5). Because the permutation representation $\mathbf{P}$ consists of a single orbit corresponding to $\mathbf{O}_h(/\mathbf{C}_{3v})$, the USCI-CF itself can be regarded as its SCI-CF. Hence, by using the data shown in the $\mathbf{O}_h(/\mathbf{C}_{3v})$-row and the $\sum$-row of Table 5, Eq. 30 is applied to this case so as to generate the following CI-CF:

$$\begin{aligned}\text{CI-CF}(\mathbf{P},\$_d) &= \frac{1}{48}b_1^8+\frac{1}{16}b_2^4+\frac{1}{8}b_2^4+\frac{1}{16}c_2^4+\frac{1}{8}a_1^4c_2^2+\frac{1}{48}c_2^4+\frac{1}{6}b_1^2b_3^2+\frac{1}{8}b_4^2+\frac{1}{8}c_4^2+\frac{1}{6}c_2c_6\\ &= \frac{1}{48}b_1^8+\frac{3}{16}b_2^4+\frac{1}{6}b_1^2b_3^2+\frac{1}{8}b_4^2+\frac{1}{12}c_2^4+\frac{1}{6}c_2c_6+\frac{1}{8}a_1^4c_2^2+\frac{1}{8}c_4^2. \qquad (40)\end{aligned}$$

Let us consider an inventory of proligands:

$$\mathbf{L}=\{\mathrm{H},\mathrm{X},\mathrm{Y},\mathrm{Z};\ \mathrm{p},\overline{\mathrm{p}};\ \mathrm{q},\overline{\mathrm{q}}\}, \qquad (41)$$

where H, X, Y, and Z are achiral proligands in isolation, while p, q, $\overline{\mathrm{p}}$, and $\overline{\mathrm{q}}$ are chiral proligands in isolation. The pair of a letter (e.g., p) and its overlined counterpart (e.g., $\overline{\mathrm{p}}$) represents an enantiomeric pair.

According to Eqs. 36–38 of Theorem 1, we use the following inventory functions:

$$a_d = \mathrm{H}^d+\mathrm{X}^d+\mathrm{Y}^d+\mathrm{Z}^d \qquad (42)$$

$$b_d = \mathrm{H}^d+\mathrm{X}^d+\mathrm{Y}^d+\mathrm{Z}^d+\mathrm{p}^d+\overline{\mathrm{p}}^d+\mathrm{q}^d+\overline{\mathrm{q}}^d \qquad (43)$$

$$c_d = \mathrm{H}^d+\mathrm{X}^d+\mathrm{Y}^d+\mathrm{Z}^d+2\mathrm{p}^{d/2}\overline{\mathrm{p}}^{d/2}+2\mathrm{q}^{d/2}\overline{\mathrm{q}}^{d/2}. \qquad (44)$$

In order to enumerate cubane derivatives as 3D-structural isomers, these ligand-inventory functions (Eqs. 42–44) are introduced into the right-hand side of Eq. 40. The expansion of the resulting function gives the following generating function:

$$\begin{aligned}g &= \mathrm{H}^8+\mathrm{H}^7\mathrm{X}+\mathrm{H}^7\mathrm{Y}+\mathrm{H}^7\mathrm{Z}+\frac{1}{2}(\mathrm{H}^7\mathrm{p}+\mathrm{H}^7\overline{\mathrm{p}})+\frac{1}{2}(\mathrm{H}^7\mathrm{q}+\mathrm{H}^7\overline{\mathrm{q}})\\ &+3\mathrm{H}^6\mathrm{X}^2+3\mathrm{H}^6\mathrm{XY}+3\mathrm{H}^6\mathrm{XZ}+\frac{3}{2}(\mathrm{H}^6\mathrm{Xp}+\mathrm{H}^6\mathrm{X}\overline{\mathrm{p}})+\frac{3}{2}(\mathrm{H}^6\mathrm{Xq}+\mathrm{H}^6\mathrm{X}\overline{\mathrm{q}})\\ &+3\mathrm{H}^6\mathrm{Y}^2+3\mathrm{H}^6\mathrm{YZ}+\frac{3}{2}(\mathrm{H}^6\mathrm{Yp}+\mathrm{H}^6\mathrm{Y}\overline{\mathrm{p}})+\frac{3}{2}(\mathrm{H}^6\mathrm{Yq}+\mathrm{H}^6\mathrm{Y}\overline{\mathrm{q}})+3\mathrm{H}^6\mathrm{Z}^2\\ &+\frac{3}{2}(\mathrm{H}^6\mathrm{Zp}+\mathrm{H}^6\mathrm{Z}\overline{\mathrm{p}})+\frac{3}{2}(\mathrm{H}^6\mathrm{Zq}+\mathrm{H}^6\mathrm{Z}\overline{\mathrm{q}})+\frac{3}{2}(\mathrm{H}^6\mathrm{p}^2+\mathrm{H}^6\overline{\mathrm{p}}^2)+3\mathrm{H}^6\mathrm{p}\overline{\mathrm{p}}\\ &+\frac{3}{2}(\mathrm{H}^6\mathrm{pq}+\mathrm{H}^6\overline{\mathrm{pq}})+\frac{3}{2}(\mathrm{H}^6\mathrm{p}\overline{\mathrm{q}}+\frac{3}{2}\mathrm{H}^6\overline{\mathrm{p}}\mathrm{q})+\frac{3}{2}(\mathrm{H}^6\mathrm{q}^2+\mathrm{H}^6\overline{\mathrm{q}}^2)+3\mathrm{H}^6\mathrm{q}\overline{\mathrm{q}}\\ &+3\mathrm{H}^5\mathrm{X}^3+6\mathrm{H}^5\mathrm{X}^2\mathrm{Y}+6\mathrm{H}^5\mathrm{X}^2\mathrm{Z}+\frac{7}{2}(\mathrm{H}^5\mathrm{X}^2\mathrm{p}+\mathrm{H}^5\mathrm{X}^2\overline{\mathrm{p}})+\frac{7}{2}(\mathrm{H}^5\mathrm{X}^2\mathrm{q}+\mathrm{H}^5\mathrm{X}^2\overline{\mathrm{q}})\\ &+6\mathrm{H}^5\mathrm{XY}^2+10\mathrm{H}^5\mathrm{XYZ}+\cdots \qquad (45)\end{aligned}$$

The coefficient of each term $\mathrm{H}^h\mathrm{X}^x\mathrm{Y}^y\mathrm{Z}^z\mathrm{p}^p\overline{\mathrm{p}}^{\overline{p}}\mathrm{q}^q\overline{\mathrm{q}}^{\overline{q}}$ in the generating function g (Eq. 45) represents the number of cubane derivatives as 3D-structural isomers having h of H, x of X, y of Y, z of Z, p of p, $\overline{p}$ of $\overline{\mathrm{p}}$ q of q, and $\overline{q}$ of $\overline{\mathrm{q}}$. Such a mode of substitution can be represented by a substitution pattern $[h,x,y,z;p,\overline{p},q,\overline{q}]$, where we can presume $h\geq x\geq y\geq z$; $p\geq q$, $p\geq\overline{p}$, and $q\geq\overline{q}$ without loosing generality. For example, the substitution pattern $[5,0,0,0;2,1,0,0]$ corresponds to $\mathrm{H}^5\mathrm{p}^2\overline{\mathrm{p}}$, $\mathrm{H}^5\mathrm{p}\overline{\mathrm{p}}^2$, $\mathrm{H}^5\mathrm{q}^2\overline{\mathrm{q}}$, $\mathrm{H}^5\mathrm{q}\overline{\mathrm{q}}^2$, $\mathrm{X}^5\mathrm{p}^2\overline{\mathrm{p}}$, $\mathrm{X}^5\mathrm{p}\overline{\mathrm{p}}^2$, $\mathrm{X}^5\mathrm{q}^2\overline{\mathrm{q}}$, $\mathrm{X}^5\mathrm{q}\overline{\mathrm{q}}^2$, and so on. The

coefficients appearing in g (Eq. 45) are collected in a tabular form (column 3D of Tables 13 and 14). Each substitution pattern marked by an asterisk (e.g., [7,0,0,0;1,0,0,0]* for H^7p) has the counterpart of opposite chirality sense (e.g., [7,0,0,0;0,1,0,0]* for $H^7\overline{p}$) so that the corresponding coefficient should be duplicated to generate the number of cubane derivatives.

4.3.2 Cubane Derivatives as Steric Isomers

To count cubane derivatives as steric isomers, the cubane skeleton (**1**) is considered to belong to the point group **O**. The 8 positions of **1** generates 24 permutations on the action of the 24 elements of **O** (Eq. 21), where they construct a permutation representation $\mathbf{P}'$. The markaracter for characterizing $\mathbf{P}'$ is obtained by counting fixed positions on the action of each cyclic subgroup:

$$\widetilde{M}_{\mathbf{P}'} = (8,0,0,2,0), \tag{46}$$

which is identical of the $\mathbf{O}(/\mathbf{C}_3)$-row of Table 9. Because the permutation representation $\mathbf{P}'$ consists of a single orbit corresponding to $\mathbf{O}(/\mathbf{C}_3)$, the dominant USCI-CF itself can be regarded as its SCI-CF. Hence, by using the data shown in the $\mathbf{O}(/\mathbf{C}_3)$-row and the $\sum$-row of Table 11, Eq. 30 is applied to this case so as to generate the following CI-CF:

$$\begin{aligned} \text{CI-CF}(\mathbf{P}', b_d) &= \frac{1}{24}b_1^8 + \frac{1}{8}b_2^4 + \frac{1}{4}b_2^4 + \frac{1}{3}b_1^2b_3^2 + \frac{1}{4}b_4^2 \\ &= \frac{1}{24}b_1^8 + \frac{3}{8}b_2^4 + \frac{1}{3}b_1^2b_3^2 + \frac{1}{4}b_4^2. \end{aligned} \tag{47}$$

Note that Eq. 47 contains the SI b_d only. When the ligand inventory **L** (Eq. 41) is adopted to count cubane derivatives as steric isomers, the ligand-inventory function b_d (Eq. 43) is introduced into the right-hand side of Eq. 47. Then, the expansion of the resulting function gives the following generating function:

$$\begin{aligned} g' = {} & H^8 + H^7X + H^7Y + H^7Z + (H^7p + H^7\overline{p}) + (H^7q + H^7\overline{q}) + 3H^6X^2 + 3H^6XY + 3H^6XZ \\ & + (3H^6Xp + 3H^6X\overline{p}) + (3H^6Xq + 3H^6X\overline{q}) + 3H^6Y^2 + 3H^6YZ + (3H^6Yp + 3H^6Y\overline{p}) \\ & + (3H^6Yq + 3H^6Y\overline{q}) + 3H^6Z^2 + (3H^6Zp + 3H^6Z\overline{p}) + (3H^6Zq + 3H^6Z\overline{q}) \\ & + (3H^6p^2 + 3H^6\overline{p}^2) + 3H^6p\overline{p} + (3H^6pq + 3H^6\overline{p}\overline{q}) + (3H^6p\overline{q} + 3H^6\overline{p}q) \\ & + (3H^6q^2 + 3H^6\overline{q}^2) + 3H^6q\overline{q} + 3H^5X^3 + 7H^5X^2Y + 7H^5X^2Z + (7H^5X^2p + 7H^5X^2\overline{p}) \\ & + (7H^5X^2q + 7H^5X^2\overline{q}) + 7H^5XY^2 + 14H^5XYZ + \cdots \end{aligned} \tag{48}$$

where the coefficient of each term $H^hX^xY^yZ^zp^p\overline{p}^{\overline{p}}q^q\overline{q}^{\overline{q}}$ represents the number of cubane derivatives as steric isomers having h of H, x of X, y of Y, z of Z, p of p, $\overline{p}$ of $\overline{\text{p}}$ q of q, and $\overline{q}$ of $\overline{\text{q}}$. The coefficients appearing in g' (Eq. 48) are collected in a tabular form (column S in Tables 13 and 14). Each substitution pattern marked by an asterisk (e.g., [7,0,0,0;1,0,0,0]* for H^7p) has the counterpart (enantiomer) of opposite chirality sense (e.g., [7,0,0,0;0,1,0,0]* for $H^7\overline{p}$). The two enantiomers are counted separately as steric isomers, as shown in Tables 13 and 14 (the column S), which have been obtained by using Eq. 47.

4.3.3 Achiral Cubane Derivatives

Let A be the number of achiral derivatives and C be the number of enantiomeric pairs (a pair of enantiomers is separately counted once). Then CI-CF($\mathbf{P}, \$_d$) (Eq. 40) is equal to A + C, while

Table 13: Numbers of Cubane Derivatives with Proligands Selected from Four Achiral Proligands and Two Enantiomorphic Pairs of Chiral Proligands (Part I)

pattern	3D	S	A	E	pattern	3D	S	A	E
[8,0,0,0;0,0,0,0]	1	1	1	0					
[7,1,0,0;0,0,0,0]	1	1	1	0	[7,0,0,0;1,0,0,0]*	1/2	1	0	1/2
[6,2,0,0;0,0,0,0]	3	3	3	0	[6,0,0,0;2,0,0,0]*	3/2	3	0	3/2
[6,1,1,0;0,0,0,0]	3	3	3	0	[6,1,0,0;1,0,0,0]*	3/2	3	0	3/2
[6,0,0,0;1,1,0,0]	3	3	3	0	[6,0,0,0;1,0,1,0]*	3/2	3	0	3/2
[5,3,0,0;0,0,0,0]	3	3	3	0	[5,0,0,0;3,0,0,0]*	3/2	3	0	3/2
[5,2,1,0;0,0,0,0]	6	7	5	1	[5,2,0,0;1,0,0,0]*	7/2	7	0	7/2
[5,1,0,0;2,0,0,0]*	7/2	7	0	7/2	[5,0,0,0;2,1,0,0]*	7/2	7	0	7/2
[5,0,0,0;2,0,1,0]*	7/2	7	0	7/2	[5,1,1,1;0,0,0,0]	10	14	6	4
[5,1,1,0;1,0,0,0]*	7	14	0	7	[5,1,0,0;1,1,0,0]	9	14	4	5
[5,1,0,0;1,0,1,0]*	7	14	0	7	[5,0,0,0;1,1,1,0]*	7	14	0	7
[4,4,0,0;0,0,0,0]	6	7	5	1	[4,0,0,0;4,0,0,0]*	7/2	7	0	7/2
[4,3,1,0;0,0,0,0]	10	13	7	3	[4,3,0,0;1,0,0,0]*	13/2	13	0	13/2
[4,1,0,0;3,0,0,0]*	13/2	13	0	13/2	[4,0,0,0;3,1,0,0]*	13/2	13	0	13/2
[4,0,0,0;3,0,1,0]*	13/2	13	0	13/2	[4,2,1,1;0,0,0,0]	22	35	9	13
[4,2,1,0;1,0,0,0]*	35/2	35	0	35/2	[4,2,0,0;1,1,0,0]	23	35	11	12
[4,2,0,0;1,0,1,0]*	35/2	35	0	35/2	[4,1,1,0;2,0,0,0]*	35/2	35	0	35/2
[4,1,0,0;2,1,0,0]*	35/2	35	0	35/2	[4,1,0,0;2,0,1,0]*	35/2	35	0	35/2
[4,0,0,0;2,1,1,0]*	35/2	35	0	35/2	[4,1,1,1;1,0,0,0]*	35	70	0	35
[4,1,1,0;1,1,0,0]	41	70	12	29	[4,1,0,0;1,1,1,0]*	35	70	0	35
[4,0,0,0;1,1,1,1]	40	70	10	30					
[3,3,2,0;0,0,0,0]	17	24	10	7	[3,3,0,0;2,0,0,0]*	12	24	0	12
[3,2,0,0;3,0,0,0]*	12	24	0	12	[3,0,0,0;3,2,0,0]*	12	24	0	12
[3,0,0,0;3,0,2,0]*	12	24	0	12	[3,3,1,1;0,0,0,0]	30	48	12	18
[3,3,1,0;1,0,0,0]*	24	48	0	24	[3,3,0,0;1,1,0,0]	28	48	8	20
[3,3,0,0;1,0,1,0]*	24	48	0	24	[3,1,1,0;3,0,0,0]*	24	48	0	24
[3,1,0,0;3,1,0,0]*	24	48	0	24	[3,1,0,0;3,0,1,0]*	24	48	0	24
[3,0,0,0;3,1,1,0]*	24	48	0	24	[3,0,0,0;3,0,1,1]*	24	48	0	24
[3,2,2,1;0,0,0,0]	42	70	14	28	[3,2,2,0;1,0,0,0]*	35	70	0	35
[3,2,0,0;2,1,0,0]*	35	70	0	35	[3,2,0,0;2,0,1,0]*	35	70	0	35
[3,0,0,0;2,2,1,0]*	35	70	0	35	[3,0,0,0;2,1,2,0]*	35	70	0	35
[3,2,1,1;1,0,0,0]*	70	140	0	70	[3,2,1,0;1,1,0,0]	78	140	16	62
[3,2,1,0;1,0,1,0]*	70	140	0	70	[3,2,0,0;1,1,1,0]*	70	140	0	70
[3,0,0,0;2,1,1,1]*	70	140	0	70	[3,1,1,1;1,1,0,0]	152	280	24	128
[3,1,1,1;1,0,1,0]*	140	280	0	140	[3,1,1,0;1,1,1,0]*	140	280	0	140
[3,1,0,0;1,1,1,1]	144	280	8	136					
[2,2,2,2;0,0,0,0]	68	114	22	46	[2,2,2,0;2,0,0,0]*	57	114	0	57
[2,2,0,0;2,2,0,0]	64	114	14	50	[2,2,0,0;2,0,2,0]*	57	114	0	57
[2,0,0,0;2,2,2,0]*	57	114	0	57	[2,2,2,1;1,0,0,0]*	105	210	0	105
[2,2,2,0;1,1,0,0]	118	210	26	92	[2,2,1,1;2,0,0,0]*	105	210	0	105
[2,2,1,0;2,1,0,0]*	105	210	0	105	[2,2,1,0;2,0,1,0]*	105	210	0	105
[2,2,0,0;2,1,1,0]*	105	210	0	105	[2,1,1,0;2,2,0,0]	111	210	12	99
[2,1,1,0;2,0,2,0]*	105	210	0	105	[2,1,0,0;2,2,1,0]*	105	210	0	105
[2,1,0,0;2,1,2,0]*	105	210	0	105	[2,0,0,0;2,2,1,1]	113	210	16	97
[2,0,0,0;2,1,2,1]*	105	210	0	105	[2,2,1,1;1,1,0,0]	222	420	24	198
[2,2,1,1;1,0,1,0]*	210	420	0	210	[2,2,1,0;1,1,1,0]*	210	420	0	210
[2,2,0,0;1,1,1,1]	224	420	28	196	[2,1,1,1;2,1,0,0]*	210	420	0	210
[2,1,1,1;2,0,1,0]*	210	420	0	210	[2,1,1,0;2,1,1,0]*	210	420	0	210
[2,1,1,0;2,0,1,1]*	210	420	0	210	[2,1,0,0;2,1,1,1]*	210	420	0	210
[2,1,1,1;1,1,1,0]*	420	840	0	420	[2,1,1,0;1,1,1,1]	432	840	24	408
[1,1,1,1;1,1,1,1]	864	1680	48	816					

These data appear as the coefficients of monomials in respective generating functions: column 3D (Eq. 45), column S (Eq. 48), column A (Eq. 49), and column E (Eq. 50). Each substitution pattern marked by an asterisk has the counterpart of opposite chirality sense so that the corresponding coefficient should be duplicated to generate the number of cubane derivatives.

Table 14: Numbers of Cubane Derivatives with Proligands Selected from Four Achiral Proligands and Two Enantiomorphic Pairs of Chiral Proligands (Part II)

pattern	3D	S	A	E	pattern	3D	S	A	E
[0,0,0,0;8,0,0,0]*	1/2	1	0	1/2					
[0,0,0,0;7,1,0,0]*	1/2	1	0	1/2	[0,0,0,0;7,0,1,0]*	1/2	1	0	1/2
[1,0,0,0;7,0,0,0]*	1/2	1	0	1/2					
[0,0,0,0;6,2,0,0]*	3/2	3	0	3/2	[0,0,0,0;6,0,2,0]*	3/2	3	0	3/2
[2,0,0,0;6,0,0,0]*	3/2	3	0	3/2	[0,0,0,0;6,1,1,0]*	3/2	3	0	3/2
[1,0,0,0;6,1,0,0]*	3/2	3	0	3/2	[1,0,0,0;6,0,1,0]*	3/2	3	0	3/2
[1,1,0,0;6,0,0,0]*	3/2	3	0	3/2					
[0,0,0,0;5,3,0,0]*	3/2	3	0	3/2	[0,0,0,0;5,0,3,0]*	3/2	3	0	3/2
[3,0,0,0;5,0,0,0]*	3/2	3	0	3/2	[0,0,0,0;5,2,1,0]*	7/2	7	0	7/2
[0,0,0,0;5,1,2,0]*	7/2	7	0	7/2	[1,0,0,0;5,2,0,0]*	7/2	7	0	7/2
[1,0,0,0;5,0,2,0]*	7/2	7	0	7/2	[2,0,0,0;5,1,0,0]*	7/2	7	0	7/2
[2,0,0,0;5,0,1,0]*	7/2	7	0	7/2	[2,1,0,0;5,0,0,0]*	7/2	7	0	7/2
[0,0,0,0;5,1,1,1]*	7	14	0	7	[1,0,0,0;5,1,1,0]*	7	14	0	7
[1,0,0,0;5,0,1,1]*	7	14	0	7	[1,1,0,0;5,1,0,0]*	7	14	0	7
[1,1,0,0;5,0,1,0]*	7	14	0	7	[1,1,1,0;5,0,0,0]*	7	14	0	7
[0,0,0,0;4,4,0,0]	6	7	5	1	[0,0,0,0;4,0,4,0]*	7/2	7	0	7/2
[0,0,0,0;4,3,1,0]*	13/2	13	0	13/2	[0,0,0,0;4,1,3,0]*	13/2	13	0	13/2
[1,0,0,0;4,3,0,0]*	13/2	13	0	13/2	[1,0,0,0;4,0,3,0]*	13/2	13	0	13/2
[0,0,0,0;4,2,2,0]*	11	22	0	11	[2,0,0,0;4,2,0,0]*	11	22	0	11
[2,0,0,0;4,0,2,0]*	11	22	0	11	[2,2,0,0;4,0,0,0]*	11	22	0	11
[0,0,0,0;4,2,1,1]*	35/2	35	0	35/2	[0,0,0,0;4,1,2,1]*	35/2	35	0	35/2
[1,0,0,0;4,2,1,0]*	35/2	35	0	35/2	[1,0,0,0;4,2,0,1]*	35/2	35	0	35/2
[1,1,0,0;4,2,0,0]*	35/2	35	0	35/2	[1,1,0,0;4,0,2,0]*	35/2	35	0	35/2
[2,0,0,0;4,1,1,0]*	35/2	35	0	35/2	[2,1,0,0;4,1,0,0]*	35/2	35	0	35/2
[2,1,0,0;4,0,1,0]*	35/2	35	0	35/2	[2,1,1,0;4,0,0,0]*	35/2	35	0	35/2
[1,0,0,0;4,1,1,1]*	35	70	0	35	[1,1,0,0;4,1,1,0]*	35	70	0	35
[1,1,0,0;4,0,1,1]*	35	70	0	35	[1,1,1,0;4,1,0,0]*	35	70	0	35
[1,1,1,0;4,0,1,0]*	35	70	0	35	[1,1,1,1;4,0,0,0]*	35	70	0	35
[0,0,0,0;3,3,2,0]*	12	24	0	12	[2,0,0,0;3,3,0,0]	15	24	6	9
[0,0,0,0;3,3,1,1]	30	48	12	18	[1,0,0,0;3,3,1,0]*	24	48	0	24
[1,1,0,0;3,3,0,0]	24	48	0	24	[0,0,0,0;3,2,2,1]*	35	70	0	35
[1,0,0,0;3,2,2,0]*	35	70	0	35	[2,0,0,0;3,2,1,0]*	35	70	0	35
[2,1,0,0;3,2,0,0]*	35	70	0	35	[2,1,0,0;3,0,2,0]*	35	70	0	35
[2,2,1,0;3,0,0,0]*	35	70	0	35	[1,0,0,0;3,2,1,1]*	70	140	0	70
[1,1,0,0;3,2,1,0]*	70	140	0	70	[1,1,1,0;3,2,0,0]*	70	140	0	70
[1,1,1,0;3,0,2,0]*	70	140	0	70	[2,0,0,0;3,1,1,1]*	70	140	0	70
[2,1,0,0;3,1,1,0]*	70	140	0	70	[2,1,0,0;3,0,1,1]*	70	140	0	70
[2,1,1,0;3,1,0,0]*	70	140	0	70	[2,1,1,0;3,0,1,0]*	70	140	0	70
[2,1,1,1;3,0,0,0]*	70	140	0	70	[1,1,0,0;3,1,1,1]*	140	280	0	140
[1,1,1,0;3,1,1,0]*	140	280	0	140	[1,1,1,0;3,0,1,1]*	140	280	0	140
[1,1,1,1;3,1,0,0]*	140	280	0	140	[1,1,1,1;3,0,1,0] *	140	280	0	140
[0,0,0,0;2,2,2,2]	66	114	18	48	[1,0,0,0;2,2,2,1]*	105	210	0	105
[1,1,0,0;2,2,2,0]*	105	210	0	105	[1,1,0,0;2,2,1,1]	210	420	0	210
[1,1,1,0;2,2,1,0]*	210	420	0	210	[1,1,1,0;2,1,2,0]*	210	420	0	210
[1,1,1,1;2,2,0,0]	222	420	24	198	[1,1,1,1;2,0,2,0]*	210	420	0	210
[1,1,1,0;2,1,1,1]*	420	840	0	420	[1,1,1,1;2,1,1,0]*	420	840	0	420
[1,1,1,1;2,0,1,1]*	420	840	0	420					

See the table footnote of Table 13.

the CI-CF($\mathbf{P}',b_d$) (Eq. 47) is equal to A + 2C. As a result, the CI-CF$^{(a)}$($\mathbf{P},\$_d$) for obtaining the number of achiral derivatives is evaluated to be 2CI-CF($\mathbf{P},\$_d$) − CI-CF($\mathbf{P}',b_d$) because $2(\mathrm{A}+\mathrm{C})-(\mathrm{A}+2\mathrm{C})=\mathrm{A}$. Hence, we obtain the following equation:

$$\begin{aligned}\text{CI-CF}^{(a)}(\mathbf{P},\$_d) &= 2\text{CI-CF}(\mathbf{P},\$_d)-\text{CI-CF}(\mathbf{P}',b_d)\\ &= \frac{1}{6}c_2^4+\frac{1}{3}c_2c_6+\frac{1}{4}a_1^4c_2^2+\frac{1}{4}c_4^2. \end{aligned} \tag{49}$$

As found by comparing between Eq. 40 and Eq. 49, only the terms for improper rotations appearing in Eq. 40 are adopted and multiplied by two to give Eq. 49. In other words, Eq. 49 contains no b_d. This feature holds true generally.

When the ligand inventory $\mathbf{L}$ (Eq. 41) is adopted to count achiral cubane derivatives, the ligand-inventory functions a_d and c_d (Eqs. 42 and 44) are introduced into the right-hand side of Eq. 49. Then, the expansion of the resulting function gives a generating function, from which the coefficient of each term is collected to give column A in Tables 13 and 14. The column A is also obtained from 2 times column 3D minus column S, i.e., $2g-g'$ (cf. Eqs. 45 and 48).

4.3.4 Enantiomeric Pairs of Cubane Derivatives

On a similar line to the preceding paragraphs, the CI-CF$^{(c)}$($\mathbf{P},\$_d$) for obtaining the number of enantiomeric pairs is evaluated to be CI-CF($\mathbf{P}',b_d$) − CI-CF($\mathbf{P},\$_d$) because $(\mathrm{A}+2\mathrm{C})-(\mathrm{A}+\mathrm{C})=\mathrm{C}$. Hence, we obtain the following equation:

$$\begin{aligned}\text{CI-CF}^{(e)}(\mathbf{P},\$_d) &= \text{CI-CF}(\mathbf{P}',b_d)-\text{CI-CF}(\mathbf{P},\$_d)\\ &= \frac{1}{48}b_1^8+\frac{3}{16}b_2^4+\frac{1}{6}b_1^2b_3^2+\frac{1}{8}b_4^2-\frac{1}{12}c_2^4-\frac{1}{6}c_2c_6-\frac{1}{8}a_1^4c_2^2-\frac{1}{8}c_4^2. \end{aligned} \tag{50}$$

As found by comparing between Eq. 40 and Eq. 50, the plus signs of the terms for improper rotations appearing in Eq. 40 are all changed into minus signs in Eq. 50. As found easily, this feature holds true generally.

When the ligand inventory $\mathbf{L}$ (Eq. 41) is adopted to count enantiomeric pairs of chiral cubane derivatives, the ligand-inventory functions a_d, b_d, and c_d (Eqs. 42–44) are introduced into the right-hand side of Eq. 50. Then, the expansion of the resulting function gives a generating function, from which the coefficient of each term is collected to give column E in Tables 13 and 14. The column E is also obtained from column S minus column 3D, i.e., $g'-g$ (cf. Eq. 48 minus Eq. 45).

4.3.5 Cubane Derivatives with Ligands as Graphs

When chiral proligands p/$\overline{\mathrm{p}}$ and q/$\overline{\mathrm{q}}$ are regarded as graphs $\hat{\mathrm{p}}$ and $\hat{\mathrm{q}}$, the ligand inventory $\mathbf{L}$ (Eq. 41) is reduced into

$$\mathbf{L}'=\{\mathrm{H},\mathrm{X},\mathrm{Y},\mathrm{Z},\hat{\mathrm{p}},\hat{\mathrm{q}}\} \tag{51}$$

Eq. 40 is degenerated to give:

$$\mathrm{CI}(\mathbf{P},s_d)=\frac{1}{48}s_1^8+\frac{3}{16}s_2^4+\frac{1}{6}s_1^2s_3^2+\frac{1}{8}s_4^2+\frac{1}{12}s_2^4+\frac{1}{6}s_2c_6+\frac{1}{8}s_1^4s_2^2+\frac{1}{8}s_4^2. \tag{52}$$

Eq. 47 is also degenerated to give:

$$\mathrm{CI}(\mathbf{P}',s_d)=\frac{1}{24}s_1^8+\frac{3}{8}s_2^4+\frac{1}{3}s_1^2s_3^2+\frac{1}{4}s_4^2. \tag{53}$$

Table 15: Numbers of Cubane Derivatives with Ligands as Graphs

pattern	P-G	P-S	P-A	P-E	pattern	P-G	P-S	P-A	P-E
[8,0,0,0;0,0]	1	1	1	0					
[7,1,0,0;0,0]	1	1	1	0	[7,0,0,0;1,0]	1	1	1	0
[6,2,0,0;0,0]	3	3	3	0	[6,0,0,0;2,0]	3	3	3	0
[6,1,1,0;0,0]	3	3	3	0	[6,1,0,0;1,0]	3	3	3	0
[6,0,0,0;1,1]	3	3	3	0					
[5,3,0,0;0,0]	3	3	3	0	[5,0,0,0;3,0]	3	3	3	0
[5,2,1,0;0,0]	6	7	5	1	[5,2,0,0;1,0]	6	7	5	1
[5,1,0,0;2,0]	6	7	5	1	[5,0,0,0;2,1]	6	7	5	1
[5,1,1,1;0,0]	10	14	6	4	[5,1,1,0;1,0]	10	14	6	4
[5,1,0,0;2,0]	6	7	5	1	[5,1,0,0;1,1]	10	14	6	4
[4,4,0,0;0,0]	6	7	5	1	[4,0,0,0;4,0]	6	7	5	1
[4,3,1,0;0,0]	10	13	7	3	[4,3,0,0;1,0]	10	13	7	3
[4,1,0,0;3,0]	10	13	7	3	[4,0,0,0;3,1]	10	13	7	3
[4,2,1,1;0,0]	22	35	9	13	[4,2,1,0;1,0]	22	35	9	13
[4,2,0,0;1,1]	22	35	9	13	[4,1,1,0;2,0]	22	35	9	13
[4,1,0,0;2,1]	22	35	9	13	[4,1,1,1;1,0]	38	70	6	32
[4,1,1,0;2,0]	22	35	9	13	[4,1,0,0;2,1]	22	35	9	13
[4,0,0,0;2,2]	16	22	10	6					

These data appear as the coefficients of monomials in respective generating functions: column P-G for Eq. 52, column P-S for Eq. 53, column P-A for Eq. 54, and column P-E for Eq. 55.

Eq. 49 is also degenerated to give:

$$\mathrm{CI}^{(a)}(\mathbf{P}, s_d) = \frac{1}{6}s_2^4 + \frac{1}{3}s_2 s_6 + \frac{1}{4}s_1^4 s_2^2 + \frac{1}{4}s_4^2. \tag{54}$$

Eq. 50 is also degenerated to give:

$$\mathrm{CI}^{(e)}(\mathbf{P}, s_d) = \frac{1}{48}s_1^8 + \frac{3}{16}s_2^4 + \frac{1}{6}s_1^2 s_3^2 + \frac{1}{8}s_4^2 - \frac{1}{12}s_2^4 - \frac{1}{6}s_2 s_6 - \frac{1}{8}s_1^4 s_2^2 - \frac{1}{8}s_4^2. \tag{55}$$

In accord with Eq. 51, Eqs. 42–42 are replaced by the following ligand-inventory function:

$$s_d = \mathrm{H}^d + \mathrm{X}^d + \mathrm{Y}^d + \mathrm{Z}^d + \hat{\mathrm{p}}^d + \hat{\mathrm{q}}^d. \tag{56}$$

The ligand-inventory function represented by Eq. 56 is introduced into Eq. 52, Eq. 53, Eq. 54, and Eq. 55, respectively. The resulting equations are expanded to give respective functions, whose coefficients are partly listed in Table 15, i.e., column P-G for Eq. 52, column P-S for Eq. 53, column P-A for Eq. 54, and column P-E for Eq. 55.

The coefficient of each term $\mathrm{H}^h\mathrm{X}^x\mathrm{Y}^y\mathrm{Z}^z\hat{\mathrm{p}}^{\hat{p}}\hat{\mathrm{q}}^{\hat{q}}$ in each respective generating function represents the number of cubane derivatives having h of H, x of X, y of Y, z of Z, $\hat{p}$ of $\hat{\mathrm{p}}$, and $\hat{q}$ of $\hat{\mathrm{q}}$. Such a mode of substitution can be represented by a substitution pattern $[h,x,y,z;\hat{p},\hat{q}]$, where we can presume $h \geq x \geq y \geq z$ and $\hat{p} \geq \hat{q}$ without loosing generality.

5 Illustration of Enumerated Cubane Derivatives

The data collected in Tables 13 and 14 using the ligand inventory $\mathbf{L} = \{\mathrm{H}, \mathrm{X}, \mathrm{Y}, \mathrm{Z}, \mathrm{p}, \overline{\mathrm{p}}, \mathrm{q}, \overline{\mathrm{q}}\}$ are parts of those collected in Tables 3 and 4 of Part I of the present series, which have been calculating by using a ligand inventory $\{\mathrm{H}, \mathrm{A}, \mathrm{W}, \mathrm{X}, \mathrm{Y}, \mathrm{Z}, \mathrm{p}, \overline{\mathrm{p}}, \mathrm{q}, \overline{\mathrm{q}}\}$.

As examples of cubane derivatives without chiral proligands, cubane derivatives characterized by [5,2,1,0;0,0,0,0] (H^5A^2B in place of the present H^5X^2Y) and by [4,3,1,0;0,0,0,0] (H^4A^3B in place of the present H^4X^3Y) have been already illustrated in Part I of the present series. As examples of cubane derivatives with chiral proligands, cubane derivatives characterized by [6,0,0,0;2,0,0,0] (H^6p^2) or [6,0,0,0;0,2,0,0] ($H^6\overline{p}^2$) and by [6,0,0,0;1,1,0,0] ($H^6p\overline{p}$) have been also illustrated in Part I of the present series.

Additional examples are useful to understand the methodology of stereochemistry. Figure 2 illustrates cubane derivatives with the formula H^5XYZ, where each pair of cubane derivatives linked by an underbrace indicates an enantiomeric pair. The corresponding [5,1,1,1;0,0,0,0]-row of Table 13 indicates that there exist 10 derivatives as 3D-structural isomers and 14 derivatives as Steric isomers; as well as 6 achiral derivatives and 4 enantiomeric pairs of chiral derivatives. The value 10 for 3D-structural isomers is the sum of the value 4 for enantiomeric pairs (i.e., **2** (**2a/2b**), **3** (**3a/3b**), **4** (**4a/4b**), and **5** (**5a/5b**)) and the value 6 for achiral derivatives (i.e., **6**, **7**, **8**, **9**, **10**, and **11**). Each of the derivatives collected in Figure 2 is counted once as a steric isomer so as to give the value 14, which is consistent to the column S of the [5,1,1,1;0,0,0,0]-row in Table 13.

Let us next consider cubane derivatives with the formula $H^5Xp\overline{p}$, the results of which are collected in the [5,1,0,0;1,1,0,0]-row of Table 13. In the conventional methodology of stereochemistry, such ligands p and $\overline{p}$ as contained in $H^5Xp\overline{p}$ are regarded as being different in the same way as the ligands Y and Z of H^5XYZ (cf. Figure 2). The methodology has been successively used in the priority rules of the Cahn-Ingold-Prelog (CIP) system [33, 34]. Because the methodology is inconsistent with actual geometric phenomena, the concept of pseudoasymmetry has been used to rationalize such inconsistency [35].

The present enumeration results collected in Figure 3 casts a new light on the inconsistency between the conventional methodology and geometric phenomena. The [5,1,0,0;1,1,0,0]-row of Table 13 indicates that there exist 9 derivatives as 3D-structural isomers and 14 derivatives as Steric isomers; as well as 4 achiral derivatives and 5 enantiomeric pairs of chiral derivatives. The value 9 for 3D-structural isomers is the sum of the value 5 for enantiomeric pairs (i.e., **16** (**16a/16b**), **17** (**17a/17b**), **18** (**18a/18b**), **19** (**19a/19b**), and **20** (**20a/20b**)) and the value 4 for achiral derivatives (i.e., **12**, **13**, **14**, and **15**). Each of the derivatives collected in Figure 2 is counted once as a steric isomer so as to give the value 14, which is consistent to the column S of the [5,1,0,0;1,1,0,0]-row of Table 13.

Pseudesymmetry is observed in a pair of **12** and **13**, which are both achiral derivatives. When our attention is focused on the carbon atom attached by the proligand X, this carbon can be regarded as exhibiting pseudoasymmetry. Thus, the permutation of p and $\overline{p}$ in **12** causes isomerization into **13**, where both **12** and **13** are achiral and they are diastereomeric (not enantiomeric). Compare the diastereomeric pair of **12** and **13** (Figure 3) with the enantiomeric pair of **2a** and **2b** (Figure 2) which are interchangeable by the permutation of Y and Z. The diastereomeric pair of **14** and **15** (Figure 3) and the enantiomeric pair of **3a** and **3b** (Figure 2) can be discussed on a similar line. Obviously, the concept of pseudoasymmetry stems from an implicit equalization of the permutations of two types (between p and $\overline{p}$ and between Y and Z), although the geometric meanings of the permutations are different from each other. Geometrically speaking, the proligands p and $\overline{p}$ in **12** (or **13**) are equivalent under the point group $\mathbf{O}_h$, while the proligands Y and Z in **3a** and **3b** are non-equivalent under the the point group $\mathbf{O}_h$.

The cubane derivatives collected in Figure 3 can be further categorized into stereoisomers, which are categorized into a common graph (constitutional isomers), as surrounded by a frame, i.e., a set of **12** and **13**, a set of **14** and **15**, a set of **16** (**16a/16b**) and **17** (**17a/17b**), a set of **18**

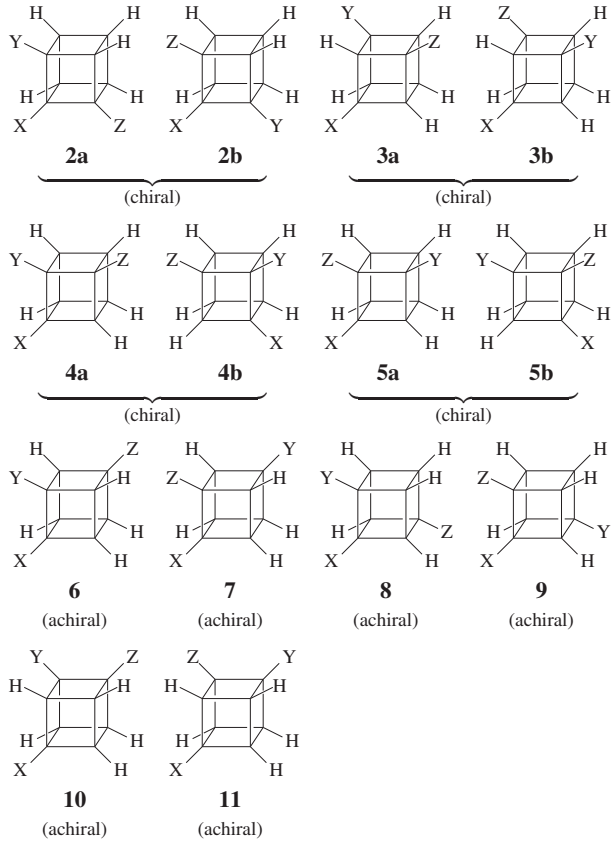

Figure 2: Cubane derivatives with H^5XYZ ([5,1,1,1;0,0,0,0])

(**18a/18b**), a set of **19** (**19a/19b**), and a set of **20** (**20a/20b**). Because each set surrounded by a frame corresponds to a common graph by putting $\hat{p} = p = \overline{p}$, this feature is rationalized in the [5,1,0,0;2,0]-column ($H^5X\hat{p}^2$) of Table 15. The value 6 of the P-G column is consistent with the number of inequivalent stereoisomers, which is found as the number of frames corresponding to the respective graphs.

6 Conclusions

The markaracter method proposed by us [26, 27] is applied to combinatorial enumeration of cubane derivatives by staring from a cubane skeleton of the point group $\mathbf{O}_h$. After the markaracter table of $\mathbf{O}_h$, its inverse, the dominant USCI-CF (unit subduced cycle indices with chirality

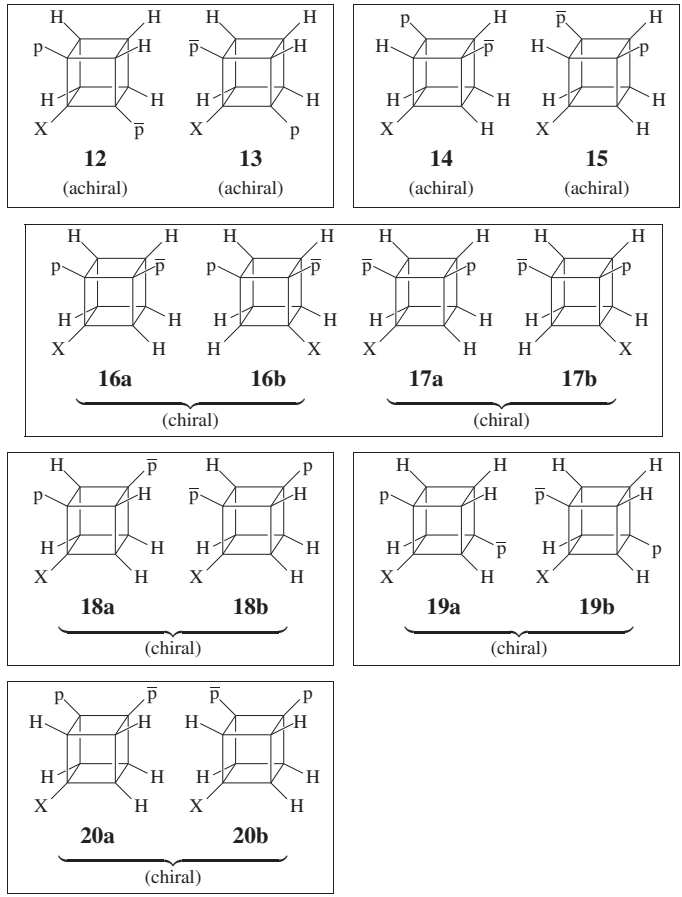

Figure 3: Cubane derivatives with $H^5Xp\overline{p}$ ([5,1,0,0;1,1,0,0])

fittingness) table of $\mathbf{O}_h$, and the non-dominant USCI-CF table of $\mathbf{O}_h$ are prepared, the markaracter method is applied to generate SCI-CFs (subduced cycle indices with chirality fittingness), which are in turn used to prepare a CI-CF (cycle indices with chirality fittingness). Thereby, cubane derivatives with chiral and achiral proligands are counted as 3D structural isomers. The markaracter table and related tables for the point group $\mathbf{O}$ are prepared so as to count cubane derivatives as steric isomers. These results are further used to count achiral cubane derivatives and enantiomeric pairs.

References

[1] J.-P. Serre, “Linear representations fo finite groups,” Springer-Verlag, New York (1977).
[2] C. W. Curtis and I. Reiner, “Representation theory of finite groups and associative algebras,” John Wikey & Sons, New York (1962).
[3] W. Burnside, “Theory of Groups of Finite Order,” 2nd ed., Cambridge University Press, Cambridge (1911).
[4] M. Oshima, “Group Theory (Gunron),” Kyoritu, Tokyo (1954).
[5] M. J. Collins, “Representations and Characters of Finite Groups,” Cambridge Univ. Press, Cambridge (1990).
[6] G. James and M. Liebeck, “Representations and Characters of Groups,” Cambridge Univ. Press, Cambridge (1993).
[7] H. H. Jaffé and M. Orchin, “Symmetry in Chemistry,” Wiley, Chichester (1965).
[8] L. H. Hall, “Group Theory and Symmetry in Chemistry,” McGraw-Hill, New York (1969).
[9] F. A. Cotton, “Chemical Applications of Group Theory,” Wiley-International, New York (1971).
[10] B. S. Tsukerblat, “Group Theory in Chemistry and Spectroscopy,” Academic, New York (1994).
[11] M. Hamermesh, “Group Theory and its Application to Physical Problems,” Dover, New York (1962).
[12] S. F. A. Kettle, “Symmetry and Structure,” Wiley, Chichester (1985).
[13] W. Ludwig and C. Falter, “Symmetries in Physics,” Springer-Verlag, Berlin Heidelberg (1988).
[14] M. F. C. Ladd, “Symmetry in Molecules and Crystals,” Ellis Horwood, Chichester (1989).
[15] T. Oyama, “Finite Permutation Groups (Yugen-Chikan-Gun),” Shokabo, Tokyo (1981).
[16] P. J. Cameron, “Permutation Groups,” Cambridge Univ. Press, Cambridge (1999).
[17] J. Sheehan, *Canad. J. Math.*, **20**, 1068–1076 (1968).
[18] W. Hässelbarth, *Theor. Chim. Acta*, **67**, 339–367 (1985).
[19] C. A. Mead, *J. Amer. Chem. Soc.*, **109**, 2130–2137 (1987).
[20] S. Fujita, *Theor. Chim. Acta*, **76**, 247–268 (1989).
[21] S. Fujita, “Symmetry and Combinatorial Enumeration in Chemistry,” Springer-Verlag, Berlin-Heidelberg (1991).
[22] S. Fujita, *J. Am. Chem. Soc.*, **112**, 3390–3397 (1990).
[23] S. Fujita, *J. Math. Chem.*, **5**, 121–156 (1990).
[24] S. Fujita, *Bull. Chem. Soc. Jpn.*, **63**, 203–215 (1990).
[25] S. Fujita, “Diagrammatical Approach to Molecular Symmetry and Enumeration of Stereoisomers,” University of Kragujevac, Faculty of Science, Kragujevac (2007).
[26] S. Fujita, *Theor. Chem. Acta*, **91**, 291–314 (1995).
[27] S. Fujita, *Theor. Chem. Acta*, **91**, 315–332 (1995).
[28] S. Fujita, *J. Math. Chem.*, **30**, 249–270 (2001).
[29] S. Fujita, *Bull. Chem. Soc. Jpn.*, **73**, 329–339 (2000).
[30] S. Fujita, *Polyhedron*, **12**, 95–110 (1993).
[31] M. B. Monagan, K. O. Geddes, K. M. Heal, G. Labahn, S. M. Vorkoetter, J. McCarron, and P. DeMarco, “Maple 9. Advanced Programming Guide,” Maplesoft, Waterloo (2003).
[32] S. Fujita, *Theor. Chem. Acc.*, **113**, 73–79 (2005).
[33] R. S. Cahn, C. K. Ingold, and V. Prelog, *Angew. Chem. Int. Ed. Eng.*, **5**, 385–415 (1966).
[34] V. Prelog and G. Helmchen, *Angew. Chem. Int. Ed. Eng.*, **21**, 567–583 (1982).

[35] V. Prelog and G. Helmchen, *Helv. Chim. Acta*, **55**, 2581–2598 (1972).

Appendix

Maple Program for Generating the Data of Table 5

```
#markarac04.mpl
#USCI-CFs for non-dominant part
#read "c:/fujita0/markarac04.mpl";

#with(linalg); #already loaded Maple 9.5
MOh := matrix(10,10,
[[48,0,0,0,0,0,0,0,0,0],[24,8,0,0,0,0,0,0,0,0],
[24,0,4,0,0,0,0,0,0,0],[24,0,0,8,0,0,0,0,0,0],
[24,0,0,0,4,0,0,0,0,0],[24,0,0,0,0,24,0,0,0,0],
[16,0,0,0,0,0,4,0,0,0],[12,4,0,0,0,0,0,4,0,0],
[12,4,0,0,0,0,0,0,4,0],[8,0,0,0,0,8,2,0,0,2]]);

InvMOh := matrix(10,10,
[[1/48,0,0,0,0,0,0,0,0,0],[-1/16,1/8,0,0,0,0,0,0,0,0],
[-1/8,0,1/4,0,0,0,0,0,0,0],[-1/16,0,0,1/8,0,0,0,0,0,0],
[-1/8,0,0,0,1/4,0,0,0,0,0],[-1/48,0,0,0,0,1/24,0,0,0,0],
[-1/12,0,0,0,0,0,1/4,0,0,0],[0,-1/8,0,0,0,0,0,1/4,0,0],
[0,-1/8,0,0,0,0,0,0,1/4,0],
[1/12,0,0,0,0,-1/6,-1/4,0,0,1/2]]);

ndUSCIcf := proc(m::vector)
local v, USCIcf;
v:=evalm(m &* InvMOh);
USCIcf:=vector(10);
USCIcf[1]:=sort(
(b1^(48*v[1]))*(b1^(24*v[2]))*(b1^(24*v[3]))*(b1^(24*v[4]))*
(b1^(24*v[5]))*(b1^(24*v[6]))*(b1^(16*v[7]))*(b1^(12*v[8]))*
(b1^(12*v[9]))*(b1^(8*v[10])),[b1,b2]);
USCIcf[2]:=sort(
(b2^(24*v[1]))*(b1^(8*v[2]))*(b2^(8*v[2]))*(b2^(12*v[3]))*
(b2^(12*v[4]))*(b2^(12*v[5]))*(b2^(12*v[6]))*
(b2^(8*v[7]))*(b1^(4*v[8]))*(b2^(4*v[8]))*
(b1^(4*v[9]))*(b2^(4*v[9]))*(b2^(4*v[10])),[b1,b2]);
USCIcf[3]:=sort(
(b2^(24*v[1]))*(b2^(12*v[2]))*(b1^(4*v[3]))*(b2^(10*v[3]))*
(b2^(12*v[4]))*(b2^(12*v[5]))*(b2^(12*v[6]))*
(b2^(8*v[7]))*(b2^(6*v[8]))*(b2^(6*v[9]))*
(b2^(4*v[10])),[b1,b2]);
USCIcf[4]:=sort(
(c2^(24*v[1]))*(c2^(12*v[2]))*(c2^(12*v[3]))*
(a1^(8*v[4]))*(c2^(8*v[4]))*(c2^(12*v[5]))*
(c2^(12*v[6]))*(c2^(8*v[7]))*(c2^(6*v[8]))*
(c2^(6*v[9]))*(c2^(4*v[10])),[a1,c2]);
USCIcf[5]:=sort(
(c2^(24*v[1]))*(c2^(12*v[2]))*(c2^(12*v[3]))*
(c2^(12*v[4]))*(a1^(4*v[5]))*(c2^(10*v[5]))*
(c2^(12*v[6]))*(c2^(8*v[7]))*(c2^(6*v[8]))*
(c2^(6*v[9]))*(c2^(4*v[10])),[a1,c2]);
USCIcf[6]:=sort(
(c2^(24*v[1]))*(c2^(12*v[2]))*(c2^(12*v[3]))*
(c2^(12*v[4]))*(c2^(12*v[5]))*(a1^(24*v[6]))*
(c2^(8*v[7]))*(c2^(6*v[8]))*
(c2^(6*v[9]))*(a1^(8*v[10])),[a1,c2]);
```

```
USCIcf[7]:=sort(
(b3^(16*v[1]))*(b3^(8*v[2]))*(b3^(8*v[3]))*
(b3^(8*v[4]))*(b3^(8*v[5]))*(b3^(8*v[6]))*
(b1^(4*v[7]))*(b3^(4*v[7]))*
(b3^(4*v[8]))*(b3^(4*v[9]))*
(b1^(2*v[10]))*(b3^(2*v[10])),[b1,b2,b3]);
USCIcf[8]:=sort(
(b4^(12*v[1]))*(b2^(4*v[2]))*(b4^(4*v[2]))*
(b4^(6*v[3]))*(b4^(6*v[4]))*(b4^(6*v[5]))*
(b4^(6*v[6]))*(b4^(4*v[7]))*
(b1^(4*v[8]))*(b4^(2*v[8]))*
(b2^(2*v[9]))*(b4^(2*v[9]))*
(b4^(2*v[10])),[b1,b2,b3,b4]);
USCIcf[9]:=sort(
(c4^(12*v[1]))*(c2^(4*v[2]))*(c4^(4*v[2]))*
(c4^(6*v[3]))*(c4^(6*v[4]))*(c4^(6*v[5]))*
(c4^(6*v[6]))*(c4^(4*v[7]))*
(c2^(2*v[8]))*(c4^(2*v[8]))*
(a1^(4*v[9]))*(c4^(2*v[9]))*
(c4^(2*v[10])),[a1,c2,c4]);
USCIcf[10]:=sort(
(c6^(8*v[1]))*(c6^(4*v[2]))*(c6^(4*v[3]))*
(c6^(4*v[4]))*(c6^(4*v[5]))*(a3^(8*v[6]))*
(c2^(2*v[7]))*(c6^(2*v[7]))*
(c6^(2*v[8]))*(c6^(2*v[9]))*
(a1^(2*v[10]))*(a3^(2*v[10])),[a1,a3,c2,c6]);

printf("%a, %a, %a, %a, %a, %a, %a, %a, %a, %a",
USCIcf[1],USCIcf[2],USCIcf[3],USCIcf[4],
USCIcf[5],USCIcf[6],USCIcf[7],USCIcf[8],
USCIcf[9],USCIcf[10]);
end proc:

m:= vector([12,12,0,0,0,0,0,0,0,0]); ndUSCIcf(m);
m:= vector([12,4,4,0,0,0,0,0,0,0]); ndUSCIcf(m);
m:= vector([12,4,0,8,0,0,0,0,0,0]); ndUSCIcf(m);
m:= vector([12,4,0,0,4,0,0,0,0,0]); ndUSCIcf(m);
m:= vector([12,0,2,4,2,0,0,0,0,0]); ndUSCIcf(m);
m:= vector([12,4,0,4,0,12,0,0,0,0]); ndUSCIcf(m);
m:= vector([12,0,2,0,2,12,0,0,0,0]); ndUSCIcf(m);

m:= vector([8,0,4,0,0,0,2,0,0,0]); ndUSCIcf(m);
m:= vector([8,0,0,0,4,0,2,0,0,0]); ndUSCIcf(m);
m:= vector([6,6,2,0,0,0,0,2,0,0]); ndUSCIcf(m);
m:= vector([6,2,0,4,2,0,0,2,0,0]); ndUSCIcf(m);
m:= vector([6,2,0,2,0,6,0,2,2,0]); ndUSCIcf(m);
m:= vector([6,6,0,0,2,0,0,0,2,0]); ndUSCIcf(m);
m:= vector([6,2,2,4,0,0,0,0,2,0]); ndUSCIcf(m);
m:= vector([6,6,0,6,0,6,0,0,0,0]); ndUSCIcf(m);
m:= vector([6,2,2,2,2,6,0,0,0,0]); ndUSCIcf(m);

m:= vector([4,4,0,0,0,0,4,0,0,0]); ndUSCIcf(m);
m:= vector([4,0,2,0,2,4,1,0,0,1]); ndUSCIcf(m);

m:= vector([3,3,1,3,1,3,0,1,1,0]); ndUSCIcf(m);

m:= vector([2,2,2,0,0,0,2,2,0,0]); ndUSCIcf(m);
m:= vector([2,2,0,2,0,2,2,0,0,2]); ndUSCIcf(m);
m:= vector([2,2,0,0,2,0,2,0,2,0]); ndUSCIcf(m);

m:= vector([1,1,1,1,1,1,1,1,1,1]); ndUSCIcf(m);
```